REGISTERED NO. M. 3121

UNIVERSITY OF MICHIGAN
FEB 2[illegible] 1955
PHYSICS LIBRARY

PROCEEDINGS

OF THE

INDIAN ACADEMY OF SCIENCES

VOL. XL] *SECTION A* [NO. 6

DECEMBER 1954

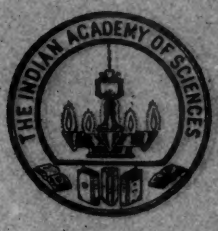

Price Rs. 2 or 3 Sh. *Annual Subscription Rs. 18*

PRINTED AT THE BANGALORE PRESS, BANGALORE CITY, BY C. VASUDEVA RAO,
SUPERINTENDENT AND PUBLISHED BY THE INDIAN ACADEMY OF
SCIENCES, BANGALORE.

ON THE STRUCTURE OF AMETHYST AND ITS GENESIS IN NATURE

By Sir C. V. Raman and A. Jayaraman
(*Memoir No. 62 of Raman Research Institute, Bangalore*)

Received December 14, 1954

1. Introduction

In a recent issue of these *Proceedings*,[1] evidence was presented showing that amethyst is a crystalline solid akin to colourless quartz in its structure but with a different electronic configuration which is assignable to a lower symmetry class and giving X-ray reflection intensities differing from those of quartz. These findings are supported and illumined by the results reported in a paper by S. Pancharatnam[2] published simultaneously with ours. It was shown by him that amethyst is optically biaxial and exhibits trichroism, and that when these two properties are considered together, they indicate only monoclinic symmetry for amethyst, whereas colourless quartz has trigonal symmetry. Interesting relationships however exist between amethyst and the associated quartz in their crystallographic orientations. The monoclinic symmetry axis of amethyst coincides with one of the electrical axes of quartz; the latter is different for the three colour sectors usually appearing in a crystal of amethystine quartz. The right or left-handedness of the crystal determines which of the two axes meeting a particular rhombohedral face is the symmetry axis of the amethyst in the colour-sector contiguous to that face. For vibrations along the monoclinic symmetry axis, the colour of the transmitted light is a light orange with a maximum of absorption in the spectrum near 5000 Å. For vibrations along the two other colour axes, the colour of the transmitted light is respectively blue with an absorption maximum near 5750 Å and a deep reddish-purple with an absorption maximum near 5250 Å. These two axes lie in a plane perpendicular to the symmetry axis and make angles of approximately 45° on either side with the *c*-axis of quartz. The latter coincides approximately with the acute bisectrix in the biaxial figure.

In the present paper, we shall report some further experimental results and proceed to make some suggestions regarding the structure of amethyst which offer a pathway to the explanation of its optical behaviour. Some

evidence is also presented which throws light on the very interesting question of the genesis of amethyst in nature.

2. AMETHYST AND SMOKY QUARTZ

With our earlier paper, photographs were reproduced to illustrate the very significant difference between amethyst and smoky quartz in their optical behaviour, *viz.*, that the former does not exhibit the diffusion so conspicuously evident in the case of the latter when traversed by a pencil of light. We have since obtained somewhat better pictures exhibiting this difference, which are reproduced as Figs. 1, 2, 3 and 4 in Plate XVII accompanying the present paper. For recording these photographs, the specimen under study was immersed in a flat-sided cell containing freshly distilled benzyl alcohol which has a refractive index nearly the same as that of quartz. A narrow beam of sunlight traversed the specimen thus immersed and the cell was viewed transversely and photographed with approximately the same exposure time in each case.

Figure 1 is a record obtained with a polished cylinder of optically clear Brazilian quartz. Visually, a faint blue track could be seen, but a much longer exposure time than that actually employed would have been necessary to record the same. The track of the beam in the benzyl alcohol however appears with great intensity.

Figure 2 is a similar record obtained with a polished sphere of smoky quartz which had been specially prepared from a rounded pebble from Ceylon presented to us by Dr. C. S. Pichamuthu to whom our thanks are due. The specimen was only faintly smoky, but nevertheless, as can be seen from Fig. 2, the track of the beam was conspicuously visible, and was many times brighter than the track in colourless quartz as seen visually. The progressive extinction of the incident beam in traversing the smoky quartz is very evident in Fig. 2. The scattered light is, of course, also enfeebled by absorption before its emergence.

Figures 3 and 4 are slightly enlarged reproductions of photographs obtained with two strongly coloured amethyst gem-stones in our possession. In neither case does the interior of the crystal exhibit any visible evidence of the passage of the light through it. The track of the beam in the benzyl alcohol is weaker after its passage through the amethyst than before it. This is to be expected in view of the absorption of light in the crystal which is strongest in the green, yellow and orange regions of the spectrum. A similar absorption would necessarily also operate on the scattered light, if any, before

it emerges in a transverse direction. But since the shorter wave-lengths in the visible spectrum are the least absorbed in amethyst and would also be the strongest in the light scattered by it and since also, the thickness needing to be traversed is relatively small owing to the particular shape of our specimens, such absorption would in no way have prevented the observation of a Tyndall effect, had this been actually present.

3. The Diamagnetic Behaviour of Amethyst

In view of a recent report which appeared in the columns of *Nature*[3] claiming that strongly coloured specimens of amethyst are paramagnetic and that the colour of amethyst is accordingly to be ascribed to the presence of ferric iron in it, we thought it worthwhile even before our first paper was published to make some qualitative tests to ascertain the true position regarding this matter. In view of the very high paramagnetism exhibited by oxides of iron, very small percentages of the same present as included material would suffice to give wholly misleading results regarding the magnetic behaviour of amethyst. It is accordingly of the highest importance to use selected specimens shown by rigorous optical test to be free from such inclusions. In our preliminary observations, we used the same cut and polished gemstones as those for which the densities had been determined and reported

Table I

Comparison of Diamagnetic Susceptibilities

Description	Mass in grams	Density in gm. per c.c.	Deflection in the Magnetic field: Scale divisions
Amethyst			
Intensely coloured ..	2·3394	2·651	9·1
Do. ..	1·8521	2·652	9·2
Do. ..	1·3466	2·651	9·0
Do. ..	1·0846	2·652	9·0
Do. ..	0·7137	2·650	7·0
Moderately coloured ..	2·2276	2·651	9·3
Do. ..	1·4184	2·650	8·0
Do. ..	1·2545	2·650	9·0
Lightly coloured ..	1·1595	2·653	8·7
Do. ..	1·1937	2·651	8·8
Do. ..	1·0351	2·650	9·0
Do. ..	0·7481	2·654	9·0
Colourless quartz ..	0·7481	2·650	9·1
Do. ..	0·334	..	9·1

in our first paper. Each specimen was tested in turn by attaching it to the end of a long vertical fibre and placing it in a powerful non-homogeneous magnetic field. When the electromagnet producing the field was excited, the specimen moved to a different position at which the restoring force due to its weight was balanced by the force of magnetic repulsion. The displacement produced would, in these circumstances, be determined by the mass-susceptibility of the specimen and independent of its size. Tested in this way, all the specimens listed in our earlier paper were found to be diamagnetic, and there were no noticeable differences in their behaviour in this respect.

To place the matter beyond all doubt, we have repeated these preliminary studies with improved technique. Each of the specimens under study was hung by a single rayon fibre about a metre long enclosed in a glass tube to protect it from disturbing air currents. A permanent magnet fitted with wedge-shaped pole pieces was employed to produce a non-homogeneous field. The magnet itself could be moved in such a manner that the specimen originally hanging in field-free space was transferred to a pre-determined position in a suitably chosen part of the field. The resulting displacement of the specimen was read off from the movement of the suspending fibre seen optically projected on a distant scale. Table I gives the results of measurements made with our specimens of amethyst, as also with pieces of colourless quartz. The data leave no room for doubt that, *to a first approximation, amethyst* and *quartz have the same magnetic susceptibility.* It is thus clear that the results reported in *Nature* and referred to above were based on observations made with impure and therefore unsuitable material. Incidentally, it should be mentioned that the difference between the diamagnetic susceptibility of colourless quartz along directions parallel and perpendicular to the trigonal axis as reported in the same communication is some twenty to thirty times larger than the actual difference. The latter is quite small, being indeed a little less than one half of one per cent. of the susceptibility in either direction.

4. CRYSTAL STRUCTURE OF AMETHYST

As is well known, quartz in its low and high temperature forms possesses structures which are very similar to each other, though differing in detail. In either case, the unit cell contains three SiO_2 groups, the silicon atoms being disposed in planes perpendicular to the trigonal axis of symmetry which divide the cell length into three equal parts. The oxygen atoms in high quartz are situated in three planes half-way between those containing the silicons, while in low-quartz they appear in six planes which are nearly

but (according to a recent report) not quite those of aliquot subdivision of the *c*-axis into nine equal parts. While the silicon atoms are situated in the special or symmetric positions in high-quartz, they are displaced from those positions in low-quartz and located on the three digonal axes of symmetry of the structure. The *c*-axis in either case is a screw axis, six-fold and three-fold respectively in the two cases.

If in the low-temperature form of quartz we imagine *one* of the three silicon atoms in the cell to be displaced along the digonal axis on which it lies, either towards or away from the position it would occupy in high-quartz, all the symmetry elements of the low-quartz structure would disappear, except the digonal axis in question. The modified structure would then possess only monoclinic symmetry. The same would continue to be the case if the two other silicon atoms in the cell are also displaced along their respective digonal axes, the magnitude of such displacement being the same for both but differing either in sense or magnitude or both from that of the first silicon atom. Any movement of the silicon atoms would necessarily involve movements of the oxygen atoms linked to them, as also a deformation of the oxygen tetrahedra surrounding the silicons. It would be easy however to picture such displacements of the oxygen atoms as would preserve the monoclinic symmetry contemplated above.

Thus, by a relatively simple and not improbable alteration in the structure of low-quartz, we arrive at a modification thereof possessing only monoclinic symmetry, the diad axis characteristic of such symmetry coinciding with one of the electrical axes of quartz in the undisturbed state. This is the situation which actually exists in amethyst as is shown by the study of its birefringence and pleochroism. We are therefore justified in pursuing the hypothesis and developing its consequences further. Since the surviving diad axis of symmetry may be any one of the three electrical axes of low-quartz, it follows immediately that there are three possible species of amethyst which are however different only in respect of their orientation within the colourless quartz. We thus arrive at an immediate explanation of the fact that the amethystine colour in quartz usually appears in three sectors, the orientation of its monoclinic axis altering by 120° when we pass from one sector to the next.

Figures 1 and 2 in Plate XVIII accompanying the present paper illustrate the feature referred to. These photographs were obtained of two crystals of amethyst immersed in a cell of benzyl alcohol by the light of a sodium vapour lamp transmitted through it. Figure 1 shows only two colour sectors, the absence of a third sector being readily understood as the corresponding

rhombohedral face was absent in the external form of the crystal. In Fig. 2 the three colour sectors are seen but are of very different sizes, such difference also being manifest in the external development of the corresponding rhombohedral faces. Figures 3 and 4 in Plate XVIII illustrate another feature very commonly observed in amethystine quartz. They are photographs of cut gem-stones viewed by transmitted light under immersion. Figure 3 exhibits one set of internal lamellæ consisting of alternate layers of colourless quartz and of amethyst, while in Fig. 4, two such sets are seen. In each case, the lamellæ are parallel to the rhombohedral planes in the quartz structure.

5. THE OPTICAL PROPERTIES OF AMETHYST

The change from trigonal to monoclinic symmetry would necessarily involve an alteration in the optical behaviour of amethyst as compared with that of colourless quartz. The low birefringence of quartz is explicable as arising from the approximately tetrahedral grouping of the oxygen atoms around each silicon atom, while its optical activity is a consequence of the presence of a screw axis in the structure. Since amethyst possesses only monoclinic symmetry, it should be optically biaxial, the symmetry axis being one of the optic vibration directions; the other two would lie in a plane perpendicular to it. The trigonal axis is the direction of maximum polarisability in quartz, and if the changes of polarisability produced by the change of structure are small, the same direction would continue to be the direction of maximum polarisability also in amethyst. The *c*-axis of quartz would then appear as the acute bisectrix in the biaxial figure exhibited by amethyst between crossed polaroids. It may be presumed that there would also be noticeable changes in optical activity, but these would probably not be large.

Colourless quartz is quite transparent in the visible and ultraviolet regions of the spectrum but exhibits complete opacity even in thin layers beyond 1436 A.U. Chandrasekhar[4] has shown that the optical rotatory dispersion of quartz is represented accurately by a single-term formula containing a characteristic wave-length at 926 A.U. and that the refractive dispersion is also tolerably well represented by a single-term formula of the Drude-Sellmier type containing the same wave-length, both in respect of the ordinary and extraordinary indices with only a change in the oscillator strength as between these two. It would seem therefore that the absorptions present at wave-lengths greater than 926 A.U. influence the refraction and dispersion only to a minor extent. The high transparency of quartz in the visible and ultraviolet is undoubtedly a consequence of the saturated

character of the silicon-oxygen bonds and their tetrahedral grouping in the crystal. As already remarked, the change in structure from quartz to amethyst would necessarily involve a distortion of the oxygen tetrahedra surrounding each silicon. It is not unreasonable to assume that it is this distortion which is responsible for the appearance of the absorption bands in the visible and near ultraviolet characteristic of amethyst. In view of its monoclinic symmetry, the diad axis is necessarily one of the axes of the absorption ellipsoid, the other two lying in a plane perpendicular to it. Since the edges of the oxygen tetrahedra are variously inclined to the *c*-axis of quartz, there is no reason to assume that the latter would itself be one of the colour axes, and indeed actually it is not.

6. The Genesis of Amethyst

A great collection of amethystine quartz collected by one of us some years ago from the University area near Hyderabad City in South India was available to us for examination. Certain general features observed with this material will now be described, as they are very illuminating in relation to the problem of the genesis of amethyst in nature.

An exceedingly common feature in our specimens is the appearance of an intense amethystine colour in the lower part of the crystal, the same being sharply terminated by one or more rhombohedral planes, while the upper part of the crystal is either completely colourless or exhibits a very light colour arranged in layers parallel to the same rhombohedral faces. A convenient way of exhibiting this feature is to immerse the crystal in a flat-sided cell containing benzyl alcohol and to photograph the same by the transmitted light of a sodium vapour lamp. The coloured regions appear quite dark in the resulting photograph, while the outer regions are almost completely transparent except for faint shadows due to defects in the material or the light colouration existing therein. Figures 3, 5 and 6 in Plate XX represent typical examples of this kind, the two former pictures representing the same crystal as viewed in perpendicular directions transverse to the *c*-axis.

A different and very illuminating procedure is to obtain a radiogram of the entire crystal or of a suitable section of it. Figures 1 and 2 in Plate XIX represent optical photographs of two such sections which were each about 5 mm. thick parallel to the *c*-axis, while Figs. 3 and 4 are radiograms respectively of the same specimens taken with the X-ray film quite close to the crystal. In the two former pictures, the transparent and coloured regions of quartz exhibit an intense contrast. ***No such contrast appears in the radiogram, and indeed after many trials we have been unable to observe***

the smallest difference between the X-ray transmissions of colourless and amethystine quartz. A very interesting feature is however noticeable in Figs. 3 and 4. This is the appearance of a dome or a layer, as the case may be, of material quite opaque to X-rays. This layer is viewed edgewise in the radiogram in Fig. 4 and hence appears as a single dark streak, while in Fig. 3 it is viewed sideways and appears resolved into a large number of small specks lying on the boundary between the coloured and uncoloured quartz and forming a pyramidal dome having the same shape as that boundary. This material can easily be taken out and subjected to chemical analysis and discloses itself to be ferric oxide.

The same phenomenon as seen in a thick transverse section is represented in Figs. 1 and 4 of Plate XX, the former being the optical photograph and the latter an X-radiogram. The pattern of sectors of coloured and colourless quartz which is so conspicuous in the central region of Fig. 1 is completely absent in Fig. 4, but the encompassing hexagonal ring of particles of ferric oxide shows up clearly in both the pictures. Figure 2 in Plate XX is an optical photograph of a thin transverse section cut through a part of another crystal so chosen that the dome of ferric oxide is seen in its entirety. The dark area at the centre is in fact a dense aggregate of particles of that material. To the left of it is seen a thin layer of coloured amethyst stretching out from one of the edges of the same area.

The features described and illustrated above are equally well exhibited by thousands of other specimens in our collection. The inference suggested thereby seems irresistible, namely that the transformation from colourless quartz to amethyst occurs during the growth of the crystal and that the change of structure from trigonal to monoclinic symmetry is brought about by the presence of the ferric impurities in the crystallising material and during their progressive expulsion from the growing crystal. At some stage during this process, the ferric oxide separates completely, forming aggregates and thereafter ceases to play any role, the further crystallisation appearing in the form of colourless quartz. This hypothesis completely accounts for the very close relationship between the form and extension of the colour sectors of the amethyst and the form of the encompassing dome of ferric oxide particles, as also of their very obvious relationship to the external form of the crystal.

7. SUMMARY

Amethyst is diamagnetic, its susceptibility being not measurably different from that of colourless quartz. The optical characters indicate only monoclinic symmetry, of which the diad axis coincides with one of the three electric

FIG. 1

FIG. 2

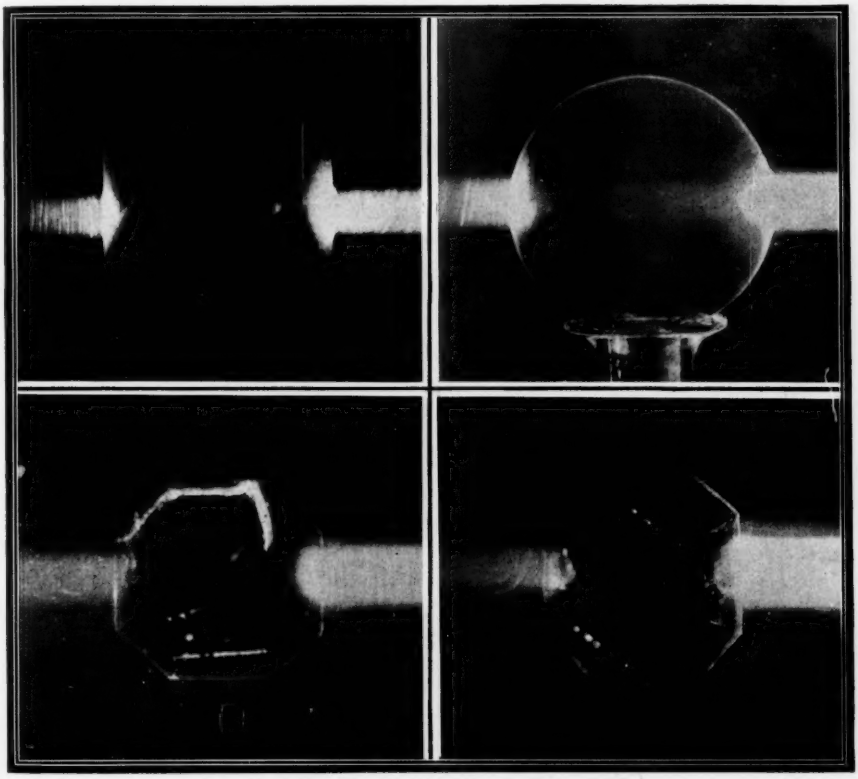

FIG. 3

FIG. 4

Scattering of Light in Smoky Quartz and Amethyst

FIG. 1

FIG. 2

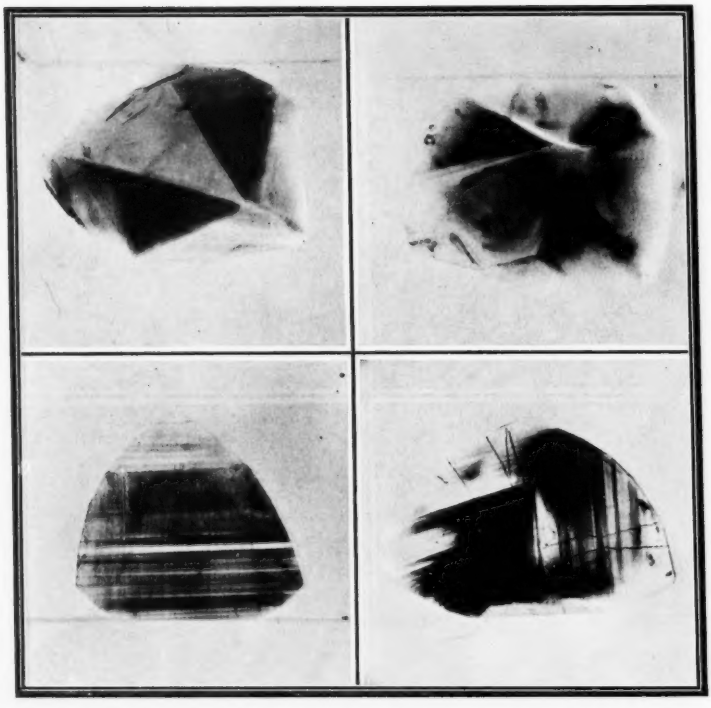

FIG. 3

FIG. 4

Colour-Sectors and Colour-Layers in Amethyst

FIG. 1

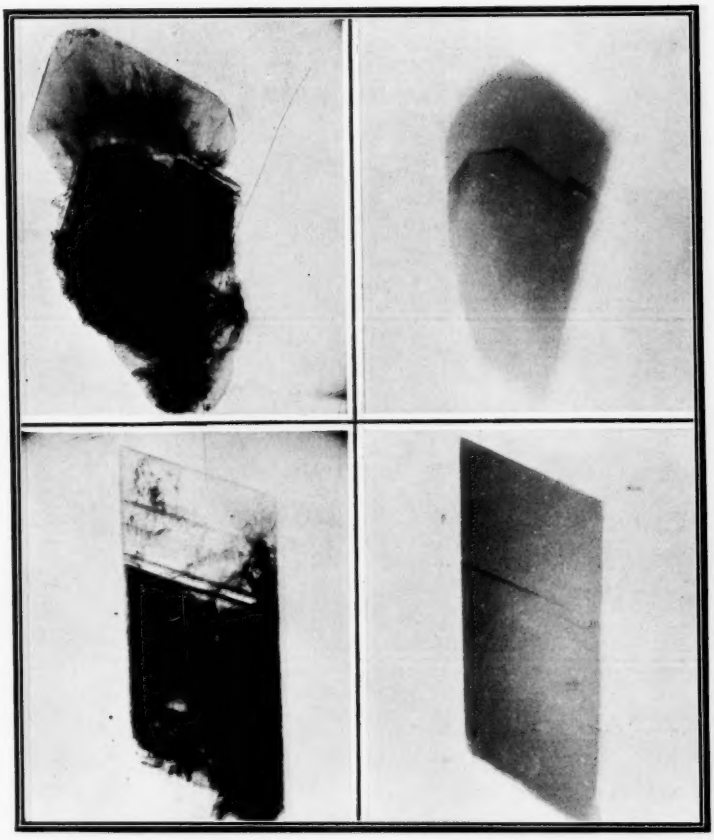

FIG. 3

FIG. 2

FIG. 4

Photographs and Radiograms of Amethyst

FIG. 1

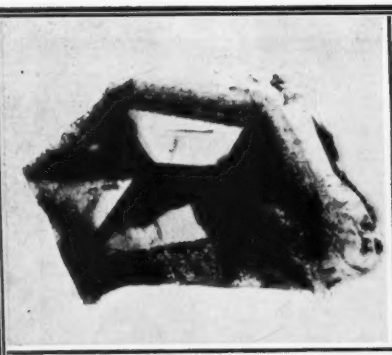

FIG. 4

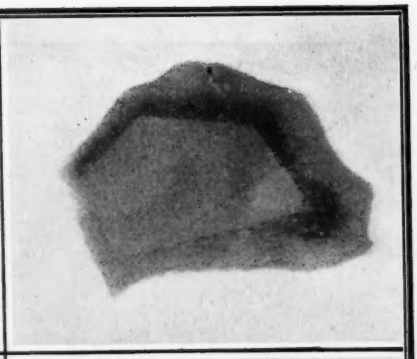

FIG. 2

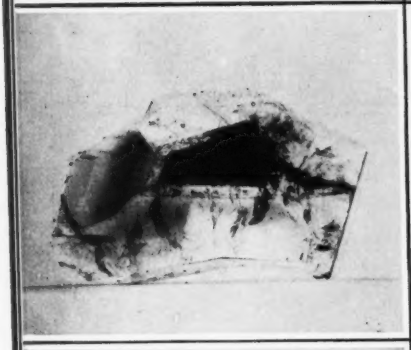

FIG. 5

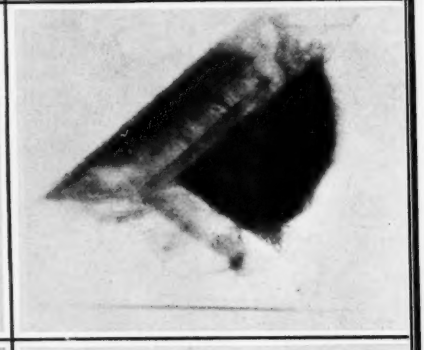

FIG. 3

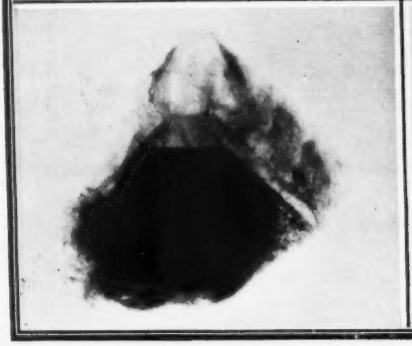

FIG. 6

Photographs and Radiogram of Amethyst

axes of the associated quartz. An immediate explanation of why three colour sectors usually appear in amethystine quartz is thus forthcoming. The nature of the modifications in structure which alter trigonal to monoclinic symmetry is indicated. A study of an extensive collection of material indicates that the change of structure occurs during the growth of the crystal from material containing ferric impurities and is consequential on the progressive elimination of these impurities which are finally deposited as a dome of discrete particles on the boundary between the amethyst and the colourless quartz.

References

1. C. V. Raman and A. Jayaraman.. *Proc. Ind. Acad. Sci.*, 1954, **40A**, 189.
2. S. Pancharatnam .. *Ibid.*, 1954, **40**, 196.
3. M. Leela .. *Nature*, 1953, **172**, 464.
4. S. Chandrasekhar .. *Proc. Ind. Acad. Sci.*, 1953, **37A**, 468.

THE FLUX OF PRIMARY COSMIC RAY NUCLEI OF ATOMIC NUMBER $Z \geqslant 2$ AT GEOMAGNETIC LATITUDE 30°

By B. Peters, F.A.Sc.

(Tata Institute of Fundamental Research, Bombay)

Received November 24, 1954

Abstract

The method of determining the primary flux of nuclei with atomic number $Z \geqslant 3$ developed by Bradt and Peters, has been extended to include all nuclei of charge $Z \geqslant 2$. It is shown that the method permits the identification of primary helium nuclei with an efficiency $\eta \geqslant 90\%$. The primary α-particle flux obtained in this way is in very good agreement with that obtained by other methods and the relative flux values for nuclei of atomic number $3 \leqslant Z \leqslant 5$ and $6 \leqslant Z \leqslant 9$ agree with previous determinations.

I. Introduction

An analysis of the relative intensity of light nuclei in the primary cosmic radiation was carried out by Bradt and Peters (1950)* with stacks of glass backed photographic emulsions exposed in balloon flights at geomagnetic latitude 30°. The experiment showed that under 20 g./cm.^{2} of residual atmosphere the relative intensity of the flux of nuclei with atomic number $3 \leqslant Z \leqslant 5$, $6 \leqslant Z \leqslant 8$ and $Z \geqslant 9$ is in the ratio of about 1 : 5 : 2.

Taking account of fragmentation processes in the upper atmosphere, Bradt and Peters concluded that the primary radiation contains few, if any, Li, Be, B nuclei near the top of the atmosphere.

This conclusion has been confirmed by Stix (1954), but has been challenged by other experimenters [Dainton, Fowler and Kent (1951, 1952), Gottstein (1953, 1954), Kaplon, Noon and Racette (1954)]. It seems, therefore, necessary to re-examine the validity of the various interpretations.

In this paper which forms part of a series dealing with this subject we shall investigate only one of the relevant questions:

What is the relative efficiency of detecting particles of various charges in the experiment of Bradt and Peters, and is it possible that the low

* This paper will be referred to as reference I.

relative intensity of Li, Be, B nuclei found by them is due to a low efficiency of detection for light nuclei compared to heavier ones?

The most direct method of answering this question consists in using the same plates and exactly the same procedure as that used in reference I, but to extend the measurements to particles of still lower ionizing power. This was done by changing the selection criteria to include primary α-particles, and determining their flux and the efficiency of their detection and identification.

Since the α-particle flux at various latitudes is known from measurements in which quite different techniques are used, the efficiency of the method can also be determined by comparison. If the method turns out to be close to 100% efficient for detecting α-particles it is safe to conclude that it has a still higher efficiency for the more than twice as heavily ionizing Lithium nuclei and the still heavier components.

The measurements described here had actually been completed in 1951, but were not analysed and published before.

II. Experimental Procedure

(*a*) *The Apparatus.*—The apparatus was the same as that used by Bradt and Peters. It consisted of a stack of 24 glass backed Kodak NTB 3 emulsions of overall dimensions $3'' \times 10''$. The plates were exposed inside a thin metal container and inserted into groves which had been machined on a milling machine. This insured that the plate spacing (d) was exactly 3 mm. Between any pair of NTB 3 emulsions was inserted a glass plate coated with less sensitive NTA emulsions. Between corresponding points on neighbouring NTB 3 emulsions there were 0·55 g./cm.^{2} of absorber (consisting mainly of glass), distributed over a distance of 3 mm.

The stack was exposed for 6 hours at geomagnetic latitude $\lambda = 30°$ under 20 g./cm.^{2} of residual atmosphere.

The emulsion thickness at the time of exposure was measured in the following way:

Tracks of heavy primary nuclei were traced through neighbouring plates. If l is their track length in one plate and L the distance between corresponding entrance points in adjacent emulsions, then the emulsion thickness at the time of exposure "a" is given by:

$$a = \frac{l}{\mathrm{L}}\, d.$$

The average value of "a" was found to be 69 μ† and its variation from the average less than 7% as estimated from the straggling of individual thickness determinations and from thickness variations measured in the processed emulsion layers.

(*b*) *Selection Criteria.*—Fig. 1 shows the position of the three plates involved in this study. The surveyed area lies in the centre of the solidly drawn portion of Plate B 445, and was 3 cm. high, and 6 cm. wide. In this area of 18 cm.^{2} all tracks were selected provided their projected length in the emulsion exceeded 400 μ and their grain density exceeded 35 grains per 75 μ. (In the experiment reference I, the corresponding value was 60 grains/75 μ.)

Plateau grain density in this emulsion was found to be 16 grains/75 μ, so that the grain density of an α-particle must be much greater than 35 grains/75 μ. The survey included, therefore, slow singly charged particles ($v/c \leqslant 0{\cdot}55$) and all multiply charged particles, whatever their energy, provided their trajectories were sufficiently parallel to the emulsion to produce the required minimum track length.

It is the purpose of this paper to show, that by a simple range criterion and without any reference to their ionizing power, relativistic α-particles (and other relativistic multiply charge nuclei) can be separated from the remaining tracks with high efficiency.

In order to show that the efficiency is high we must, however, make use of the length distribution and the grain density distribution of these tracks.

(*c*) *Range Criteria.*—A particle passing through the surveyed area of Plate B 445 may be incident from the upper hemisphere in such a direction as to traverse the stack without passing through either of the neighbouring plates (*see* Fig. 1). Particle tracks which have this position and direction, irrespective of whether they enter from the outside or originate in the stack, are put into Class O, meaning that they are not traceable into adjacent plates either into the upper or into the lower hemisphere.

A particle may be incident from the upper hemisphere in such a direction that in traversing the stack it passes through a neighbouring plate:

† This value differs from the approximate average thickness of 80 μ given in reference I. The flux values in reference I should, therefore, be increased slightly but the relative strength of various components is not affected by this correction, because its measurement does not depend on emulsion thickness.

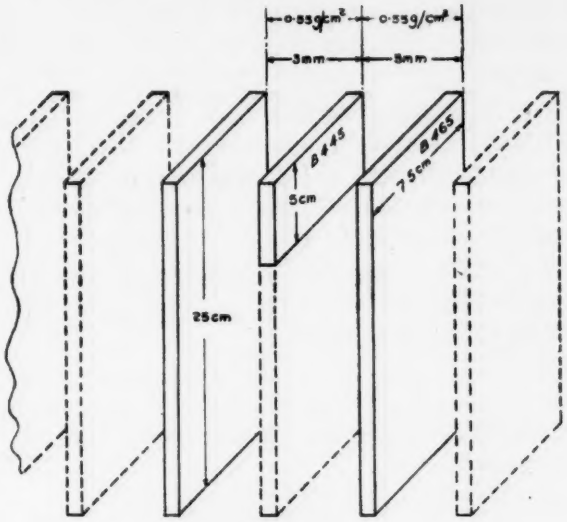

FIG. 1

(i) *before* reaching the surveyed area of Plate B 445,

(ii) *after* reaching the surveyed plate, or

(iii) *before and after* reaching the surveyed plate.

Particle tracks with the corresponding positions and directions, irrespective of whether they enter from the outside or originate inside the stack, are put into Classes U, L and UL, respectively, meaning that the tracks are traceable into the upper, the lower or the upper and the lower hemispheres.

We have tried to find the continuation in the appropriate adjacent plate or plates of all tracks which satisfied the selection criteria in Plate B 445, and which because of their geometric location fell into Classes U, L or UL. For this purpose we calculated the probable location of the track in the neighbouring plate from its direction and projected length in the surveyed area and from the known plate separation. We then surveyed an area of 6 mm.^{2} surrounding the predicted location.

A track is said to have been "followed successfully", if in the region surrounding the predicted location, a track was found whose grain density exceeded 35 grains/75 μ, and whose track length did not differ by more than 20%, either in its horizontal or vertical components, from the corresponding lengths in the surveyed area.

"Successful tracing" means, therefore, one of three things:

(i) The track is due to a fast particle of charge $Z \geqslant 2$ which did not suffer a destructive nuclear collision in the intervening glass plate.

or (ii) The track is due to a proton, deuteron or triton. If a proton, its energy must exceed 60 MeV, since a track whose length in the emulsion exceeds 400 μ, must traverse at least 3·2 g./cm.^{2} of glass to reach the neighbouring emulsion; on the other hand the energy must not exceed 200 MeV so that its grain density lies above 35 grains/75 μ.

or (iii) The tracks in the two neighbouring plates are due to two different particles and their relative position and orientation happens to satisfy our tracing criteria.

We shall show that in our comparatively light exposure (6 hours at low latitude in the stratosphere) "successful tracing" alone separates almost quantitatively the heavy primary and particularly the α-particle component from all other particles.

III. Experimental Results

(*a*) *The Efficiency of Surveying and Tracing.*—470 tracks satisfying the selection criteria were found in the 18 cm.^{2} surveyed in Plate B 445. Of these, 9 belonged to heavy primaries of atomic number $Z < 2$; their charge distribution is given in Section III (*d*).

Four tracks, due to relativistic α-particles, are strictly parallel and very closely bunched; they can be shown to arise as fragments in the collision of a heavy primary particle in the glass backing of Plate B 445, a collision of the type discussed earlier (Bradt and Peters, 1949). These four tracks are omitted from the discussion which follows.

The remaining 457 tracks are classified as to whether they are followable into the upper, or lower hemisphere, or both, as discussed above:

Class UL (followable in both hemispheres)	165 tracks
Class U (followable into upper hemispheres only) ..	54 tracks
Class L (followable into lower hemispheres only) ..	175 tracks
Class O (not followable)	63 tracks
TOTAL ..	457 tracks

We first carry out some tests to determine η_s the efficiency of the survey (selection efficiency) and to obtain at least an approximate value for η_t the efficiency with which the continuation of a track traversing two adjacent plates, could be located (tracing efficiency).

For this purpose we surveyed with identical selection criteria an additional area of 21·5 cm.² in Plate B 465, which is one of the two plates adjacent to B 445. Of the tracks found in this survey we selected those which were so oriented that they could have a continuation in the originally surveyed area of Plate B 445. There were 218 such tracks. We tried to locate their continuation in B 445 and were successful in 38 cases. We now selected among the tracks of the first survey (B 445) those which had been traced successfully into the area of the second survey (B 465) and found 34 such tracks.

33 of the tracks found and traced successfully were common to both experiments.

1 track found and traced successfully in the first survey was missed (not found) in the second survey.

5 tracks which were found and traced successfully in the second survey, were found also in the first survey, but not successfully traced.

From this we obtain an estimate for the survey efficiency η_s' and the tracing efficiency η_t' for particles with ionization *equal to or larger* than that of relativistic α-particles. If we designate by the letter n the total number of tracks which actually have segments in both the surveyed areas we get:

$$n\,\eta_s'^2\,\eta_t'^2 = 33$$

$$2n\,\eta_s'\,(1-\eta_s')\,\eta_t = 1$$

$$2n\,\eta_s'^2\,\eta_t'\,(1-\eta_t') = 5.$$

These equations yield:

$$n = 39$$

$$\eta_s' = 98{\cdot}5\%$$

$$\eta_t' = 93\%$$

If we exclude the tracks of 5 primaries heavier than helium which are included among the 33 particles common to both investigations, we obtain the corresponding efficiencies for tracks whose ionization *equals* that of relativistic α-particles:

$$\eta_s = 98 \cdot 5\%$$

$$\eta_t = 92\%$$

We confirm the high *survey* efficiency by plotting the length distribution of the 175 tracks from the original survey whose grain density is consistent with their being tracks of relativistic α-particles. In Fig. 2, the number of

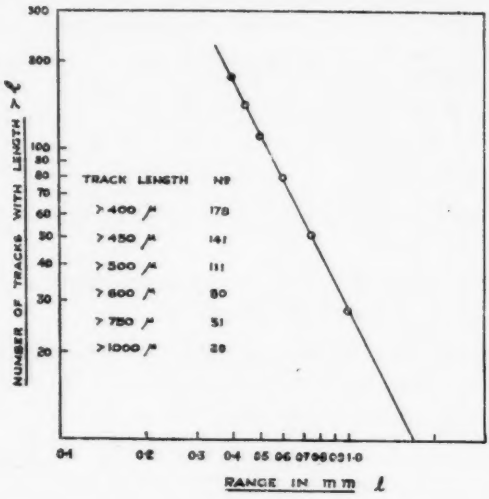

FIG. 2.

tracks whose projected length exceeds l is plotted against l. The solid line represents the relation:

$$N_{>l} \approx \frac{1}{l^2}$$

which is the expected length distribution for purely geometric reasons. Any departure of survey efficiency from 100% must primarily effect the short tracks whose length is close to the limit of 400 μ, set by the selection criteria. The fact that the experimental points at small ranges do not fall below the theoretical curve, confirms the high survey efficiency η_s deduced above.

In order to obtain independent corroboration for the high *tracing* efficiency indicated above, a more detailed analysis of the tracks is needed. We proceeded to measure the grain density of all 457 tracks in Plate 445. We also determined separately the grain density of secondary but relativistic α-particles choosing jets of parallel tracks which originated in the break up

of heavy primary nuclei in other parts of the stack. We find for relativistic α-particles a mean grain density of 51·8 grains/75 μ. In no case did their grain density fall below 45 or exceed 57 grains/75 μ in any one emulsion traversed. In the histograms (Fig. 3) where the number of particles in various

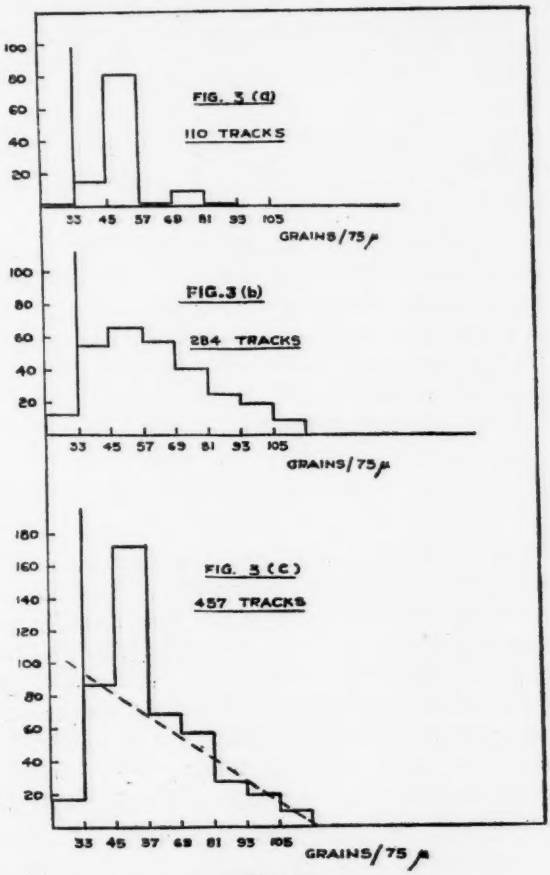

FIG. 3.

grain density intervals is shown, we have marked the abscissa in units whose width is 12 grains/75 μ, and only one of these intervals (45–57 grains/75 μ) can contain relativistic α-particles. (We are not asserting that particles in this interval of grain density are relativistic α-particles, but only that tracks which are due to relativistic α-particles must fall into this grain density interval. The arguments which follow are independent of the width of this grain

density interval and depend only on the fact that it is wide enough to accommodate all relativistic α-particle tracks.)

Fig. 3 (*a*) shows the grain density distribution in the surveyed area of all those tracks which were successfully traced in at least one neighbouring plate.

Fig. 3 (*b*) shows the grain density distribution of all those tracks which, though followable (Classes U, L, UL), were not found near the predicted position.

Fig. 3 (*c*) shows the grain density distribution of all tracks irrespective of whether they were followable or not and of whether tracing was successful or not.

Let us first consider Fig. 3 (*c*). By extrapolating the background of secondary particles through the peak of the distribution along the curve shown in the diagram we can estimate the primary α-particle flux. The peak above the extrapolated background contains 96 particles. As we shall see later the corresponding flux is in good agreement with that previously obtained by Goldfarb, Bradt and Peters (1950) by a similar method; it is also in agreement with the extrapolated curve based on α-particle flux measurements at other latitudes and by other observers.‡ We can conclude then that the detection efficiencies in all the relevant experiments were approximately equal.

Next we consider Fig. 3 *b*. It represents the grain density of all those particles which were not found near the expected position in the neighbouring emulsion, either because they failed to penetrate the intervening glass absorber or because of inefficiency in tracing. In this histogram the strong peak in the grain density interval $45 < g. < 57$ grains/75μ, has disappeared. As a whole the distribution resembles the extrapolated background curve of Fig. 3 (*c*). However, a small particle excess in the interval where relativistic α-particles must fall, indicates that some primary α-particles have stayed in this group, either because tracing was faulty or because the particles suffered a destructive collision in the intervening glass plate.

Finally we consider Fig. 3 (*a*). The histogram contains mostly particles in the grain density interval $45 < g. < 57$ grains/75μ. Since here the background of other tracks is small, extrapolation is quite accurate and we can say that not less than 70 of the 394 particles in Classes U, L and UL are identifiable by range and ionization as relativistic particles of charge $Z = 2$.

‡ See B. Peters, *The Nature of Primary Cosmic Radiation*, Vol. I—*Progress in Cosmic Ray Physics* (J. G. Wilson ed.), North-Holland Publishing Co., 1952.

For later use we must note, however, that Fig. 3 (*a*) contains 29 tracks which because of their grain density cannot be due to relativistic particles of any charge. Thus out of approximately 300 non-relativistic particles in Figs. 3 (*b*) and 3 (*c*), 29 had a continuation in an adjacent plate either because they penetrated the intervening glass or by accidental juxtaposition of two unrelated tracks. Although we cannot give this probability a meaningful physical interpretation, we shall designate it by the symbol $\epsilon \approx 10\%$ and define it as:

> the probability that a followable track due to a non-relativistic particle which satisfies our selection criteria, is "successfully followed" in the sense previously defined.

Before we can derive the tracing efficiency η_t more accurately, we still have to determine one other quantity, namely the collision probability σ. It is defined as the probability that a relativistic α-particle whose direction of motion satisfies our selection criteria will suffer between adjacent emulsions a collision in which it will lose at least one unit of charge, or be deflected through more than 5°. (A large angle deflection of a relativistic α-particle without loss of charge is highly improbable and has not yet been observed).

In order to determine the collision probability σ we make again use of secondary relativistic α-particles from the break up of primary heavy nuclei. Tracing their tracks through the stack yields a collision mean free path for relativistic α-particles in the material of our stack. It is true that its value will depend somewhat on our tracing efficiency, but since these α-particles occur in narrow bundles they can be traced with confidence and the disappearance of one of the members in a bunch between two emulsions can be established with certainty. We obtain the mean free path for collisions of relativistic α-particles in our stack: $\lambda = 50 \pm 10$ g./cm.^{2}

We now make use of the length distribution of tracks $N_{>l} \approx \frac{1}{l^2}$ which according to Fig. 2 holds for all tracks whose ionization is consistent with that of relativistic α-particles. The probability of destructive collision between adjacent emulsions is then given by:

$$\sigma = \int_{L_0}^{\infty} \frac{1 - e^{-L/\lambda}}{L^3} \, dL \Big/ \int_{L_0}^{\infty} \frac{dL}{L^3}$$

where L_0 is the amount of matter which the steepest of the acceptable particles has to traverse in going from one emulsion to the next. Using $L_0 = 3 \cdot 2$ g./cm.^{2}

as calculated before and $\lambda = 50$ g./cm.^{2} the probability of collision between emulsions becomes:

$$\sigma = 12\%$$

(*b*) *Detailed Determination of the Tracing Efficiency* η_t.—We divide the 457 tracks into 9 Groups by asking four questions:

Question 1.—Is the track traceable into the next emulsion in the direction of the upper hemisphere, yes or no?

Question 2.—Was the track "successfully traced" into the upper hemisphere, yes or no?

Question 3.—Is the track traceable into the next emulsion in the direction of the lower hemisphere, yes or no?

Question 4.—Was the track "successfully traced" into the lower hemisphere, yes or no?

Since a "no" answer to questions one and three implies automatically "no" for questions two and four respectively, we obtain 9 Groups of tracks. We designate yes by (+) and no by (−) and list below the number of tracks in each Group.

TABLE I

Class	Group	Symbol	No. of tracks found	
UL	1	+ + + +	25	
	2	+ + + −	18	
	3	+ − + +	17	
	4	+ − + −	105	165 tracks
U	5	+ + − −	5	
	6	+ − − −	49	54 tracks
L	7	− − + +	45	
	8	− − + −	130	175 tracks
O	9	− − − −	63	63 tracks
				457 tracks

The classification of tracks into different Classes is purely geometric, while the classification into Groups depends on the penetrating power of the particle involved.

It is important to realize the expected difference in composition in Groups like, for instance, Group 6 $(+ - - -)$ and Group 8 $(- - + -)$. Since all primaries enter from the upper hemisphere, Group 6 in which the particles were predicted in the upper hemisphere, but not found, cannot contain primaries unless the tracing was inefficient. Group 8, on the other hand, which contains particles predicted in the lower hemisphere, but not found, will contain some primaries which collided between plates *after* going through the surveyed area.

We can now calculate and compare with experiment the expected number of relativistic α-particles (α) and secondaries (S) in each Group in terms of three previously defined quantities, namely:

η_t, the efficiency of tracing relativistic α-particles.

$\sigma = 12\%$, the probability for a relativistic α-particle to disappear between adjacent emulsions because of collision in the glass.

$\epsilon = 10\%$, the probability for a non-relativistic particle track to have an acceptable continuation in the adjacent emulsion.

One gets:

Class UL

$$\alpha_1 = \eta_t^2 (1 - \sigma)\, \alpha_{UL} \qquad (1, a)$$

$$\alpha_2 = [\eta_t (1 - \eta_t)(1 - \sigma) + \eta_t \sigma]\, \alpha_{UL} \qquad (1, b)$$

$$\alpha_3 = \eta_t (1 - \eta_t)(1 - \sigma)\, \alpha_{UL} \qquad (1, c)$$

$$\alpha_4 = [(1 - \eta_t)^2 (1 - \sigma) + (1 - \eta_t)\sigma]\, \alpha_{UL} \qquad (1, d)$$

$$S_1 = \epsilon^2 S_{UL} = 0{\cdot}01\, S_{UL} \qquad (2, a)$$

$$S_2 = \epsilon (1 - \epsilon) S_{UL} = 0{\cdot}09\, S_{UL} \qquad (2, b)$$

$$S_3 = \epsilon (1 - \epsilon) S_{UL} = 0{\cdot}09\, S_{UL} \qquad (2, c)$$

$$S_4 = (1 - \epsilon)^2 S_{UL} = 0{\cdot}81\, S_{UL} \qquad (2, d)$$

Class U

$$\alpha_5 = \eta_t\, \alpha_U \qquad (1, e)$$

$$\alpha_6 = (1 - \eta_t)\, \alpha_U \qquad (1, f)$$

$$S_5 = \epsilon S_U = 0{\cdot}1\, S_U \qquad (2, e)$$

$$S_6 = (1 - \epsilon) S_U = 0{\cdot}9\, S_U \qquad (2, f)$$

Class L $a_7 = \eta_t (1 - \sigma) a_L$ (1, g)

$a_8 = [(1 - \eta_t)(1 - \sigma) + \sigma] a_L$ (1, h)

$S_7 = \epsilon S_L = 0{\cdot}1\, S_L$ (2, g)

$S_8 = (1 - \epsilon) S_L = 0{\cdot}9\, S_L$ (2, h)

Class O $a_9 = a_0$ (1, i)

$S_9 = S_0$ (2, i)

These formulas permit us to predict (in terms of the tracing efficiency η_t) the relative strength and composition of each Group belonging to a given geometric Class.

Let us first consider the two largest Classes namely: L and UL. Table II shows the tracks in these Classes arranged according to Groups and according to their grain density.

TABLE II

Grain Density (g./75)	Class L		Class UL			
	Group 7 (−−−++)	Group 8 (−−−+−)	Group 1 (++++)	Group 2 (+++−)	Group 3 (+−++)	Group 4 (+−+−)
< 33	−	4	..	..	1	5
33– 45	6	31	1	5	2	18
45– 57	35	30	24	9	10	18
57– 69	1	27	..	1	..	22
69– 81	3	18	..	3	3	15
81– 93	..	15	..	..	1	10
93–105	..	5	..	..	..	8
> 105	..	..	..	..	..	9
Total	45	130	25	18	17	105
Class Total	175		165			

The particles whose grain density lies below 45 or above 57 are secondaries. Any relativistic α-particles which may be in the Groups must be in the category 45–57 but, as explained before, this category will also contain secondary particles. For the purpose of comparing the predicted with the experimental strength within each Group we shall take as secondaries (S)

the number of tracks S′ whose grain density lies below 45 or above 57 multiplied by a factor $(1+f)$:

$$S = S'(1+f).$$

As the number of α-particles (α) we shall take the rest, namely, the number α′ of tracks in the grain densiy interval 45–57 minus the number of secondaries in that interval:

$$\alpha = \alpha' - fS'$$

In the case of Class L we have now the following relations:

$$a_7 = 0{\cdot}88\,\eta_t\,a_L = 35 - 10f$$
$$a_8 = (1 - 0{\cdot}88\,\eta_t)\,a_L = 30 - 100f$$

Eliminating a_L from these equations we get a relation between η_t and f, and can, therefore, plot the grain density distribution of the secondaries in Group 8 (S_8) for various assumptions about η_t.

In a similar way we can deal with Groups 1 and 4 in Class UL and plot the grain density distribution of secondaries in Group 4 for various values of η_t.

These histograms are shown in Figs. 4 (*a*) and 4 (*b*). Only the column in the grain density interval 45–57 is affected by the choice of η_t and its height is indicated for various assumed values. It is clear from these histograms that η_t must be very close to 100% and is unlikely to lie below 90%. In any case we can conclude from these histograms that $f = 0{\cdot}235$ (19% of all secondaries produce tracks in the grain density interval 45–57).

A detailed comparison of the distribution of primaries and secondaries among the Groups of a given Class has been made in Table III. In order to show how Table III was constructed we carry through a sample calculation for Groups 7 and 8 of Class L whose grain density distribution is shown in Table II.

Group 7 contains 45 tracks of which 10 fall outside the interval

$$45 - 57 \text{ g./}75\,\mu.$$

Group 8 contains 130 tracks of which 100 fall outside the interval

$$45 - 57 \text{ g./}75\,\mu.$$

The *calculated* values are obtained as follows:

$$S_L = S_L'(1+f) = 110\,(1 + 0{\cdot}235) = 136$$
$$a_L = N_L - S_L = 39$$

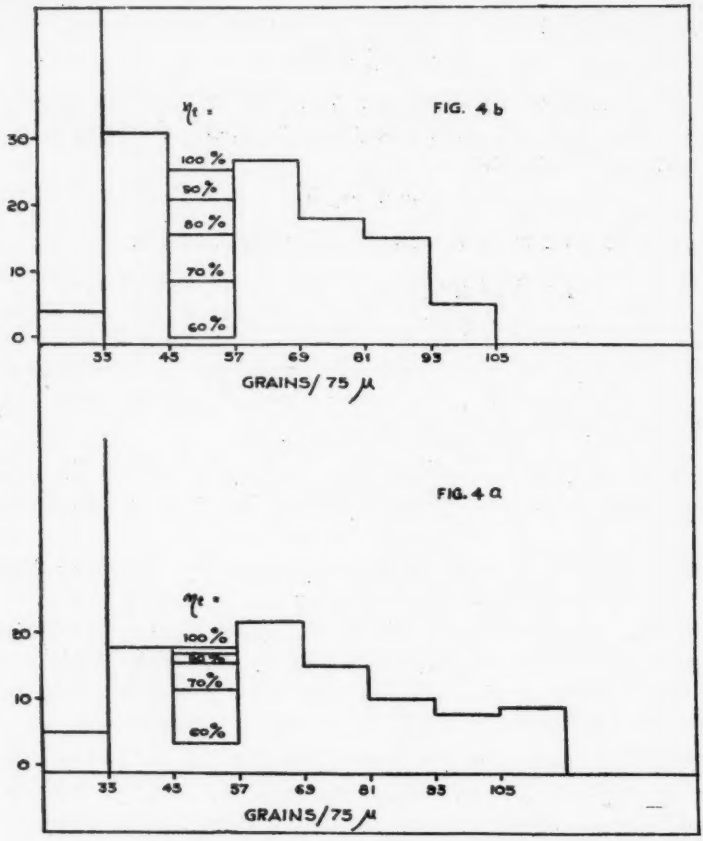

FIG. 4.

These values are inserted into eq. 1. *e*, *f*, and 2. *e*, *f*, to calculate α_7, α_8, S_7 and S_8. The calculations have been carried out for three assumed values of the scanning efficiency η_t namely, 70%, 85%, 100%, and for Classes UL, U and L. The average calculated ratio α/S for Classes UL, U and L is used to calculate α and S for Class O.

The *observed* values of α and S are obtained from the grain density distribution in each Group:

$S_7 = S_7'(1+f) = 10(1+0{\cdot}235) = 12$

$S_8 = \quad\quad = 100(1+0{\cdot}235) = 124$

$\alpha_7 = 45 - S_7 \quad = 33$

$\alpha_8 = 130 - S_8 \quad = 6.$

TABLE III

Class	Group	S		α				
		Obs.	Calc.	Obs.	Calculated $n_t = 100\%$	Calculated $n_t = 85\%$	Calculated $n_t = 70\%$	Obs.
	1 (++++)	1	1	24	32	23	15	
	2 (+++−)	11	12	7	4	8	10	
	3 (+−++)	9	12	8	..	4	7	
	4 (+−+−)	105	104	..	..	1	4	
UL	165	126	129	39	36	36	36	$\alpha/S = 0{\cdot}31$
	5 (++−−)	1	4	4	14	12	10	
	6 (+−−−)	38	36	11	..	2	4	
UL	54	39	40	15	14	14	14	$\alpha/S = 0{\cdot}38$
	7 (−−++)	12	14	33	34	29	24	
	8 (−−+−)	124	122	6	5	10	15	
L	175	136	136	39	39	39	39	$\alpha/S = 0{\cdot}29$
	9 (−−−−)	48	49	15	14	14	14	
0	63	48	49	15	14	14	14	$\alpha/S = 0{\cdot}31$

The agreement between calculated and observed values in Table III is very good for $\eta_t = 100\%$ and 85% and definitely poorer for $\eta_t = 70\%$. We conclude that the efficiency for tracing relativistic α-particles $\eta_t \gtrsim 85\%$ and that out of 457 tracks in the surveyed area 108 tracks are due to relativistic α-particles.

(*c*) *The Flux of Primary Helium Under* 20 g./*cm.*^{2} *of Residual Atmosphere at Geomagnetic Latitude* $\lambda = 30°$.—In order to determine the flux of α-particles at the top of the atmosphere, the number of relativistic α-particles identified as incident on the surveyed area must be multiplied by the geometric factor appropriate to the selection criteria and by another factor to correct for the loss by nuclear collisions in the upper atmosphere and in the glass of the stack. The calculations were carried out as discussed previously (Bradt and Peters, 1950 *a*). We have used the value of 50 g./cm.^{2} for the absorption mean free path in glass and for the absorption mean free path in air, the value of 45 g./cm.^{2} The 61 α-particles in the almost pure Groups 1, 5 and 7 were used to make these corrections and the resulting flux was increased by the factor $108 \div 61$ in order to include the primary α-particles in the remaining 6 Groups. The flux was determined separately for particles incident in the three intervals of zenith angle θ; $0 < \theta < 30°$; $30° < \theta < 60°$; $60° < \theta < 90°$ and the three values agree within statistical error. However, in order to reduce the uncertainty due to collision corrections we included in our final calculations only particles incident with a zenith angle $< 70°$.

The flux of primary α-particles at geomagnetic latitude 30° is:

$$I_\alpha = 72 \pm 15 \text{ particles per m.}^2\text{, sec., steradian.}$$

This value is in good agreement with the value 80 ± 30 particles previously obtained by Goldfarb *et al.* (1950) from the grain density distribution of tracks. It also fits accurately the previously derived empirical α-particle spectrum $I_\alpha = \frac{400}{(1+E)^{1.35}}$ valid in the latitude sensitive region. (I_α is the number of particles incident per m.^{2}, sec., ster., whose energy per nucleon exceeds E BeV.)

Because our efficiency in finding and identifying α-particles was slightly lower than 100%, our flux value ought to be increased by a small factor; on the other hand it must be lowered by 3–5% because at an atmospheric depth of 20 g./cm.^{2} there exist relativistic α-particle fragments from the fragmentation of heavier nuclei in the upper layers of the atmosphere. These corrections are smaller than the statistical error, and have, therefore, been omitted.

(*d*) *The Relative Abundance of Light Nuclei in the Primary Radiation Under* 20 *g./cm.*^{2} *of Atmosphere at Geomagnetic Latitude* $\lambda = 30°$.—We have already stated that in the course of the investigation described here, 9 tracks were identified as belonging to primaries heavier than helium. Their charge was determined by the method described in reference I. They were:

Element	No. of Tracks
Lithium	1
Beryllium	0
Boron	1
Carbon	4
Nitrogen	2
Oxygen	1
Total ..	9

Although of small statistical weight, the relative number of Lithium, Beryllium and Boron Nuclei (Li, Be, B) to those of the Carbon, Nitrogen, Oxygen nuclei (C N O Group) is the same as that obtained in reference I, and when the two results are combined one obtains at the stated atmospheric depth:

$$\frac{\text{Li, Be, B}}{\text{C N O}} = 0{\cdot}21 \pm 0{\cdot}06$$

As mentioned in the Introduction, this result disagrees with that obtained by Dainton, Fowler and Kent, by Gottstein, and with part of the experiments of Kaplen, Noon and Racette. It was the purpose of this paper to show that the discrepancy cannot be attributed to a low efficiency for identifying particles of low atomic number in the experiment of reference I. For it is clear that if an overall efficiency $\gtrsim 90\%$ is achieved for tracks made by relativistic α-particles, the efficiency for detecting heavier nuclei whose ionization is at least twice as great must be quite close to 100%. This applies particularly to the experiment of reference I, because both in the present and in the earlier experiment the greater part of scanning and tracing was carried out by the same person, Mr. R. Rickard, to whom I wish to express my gratitude at this point.

The question of efficiency in detecting and observing nuclei of various atomic numbers had been treated in great detail only in the paper of Stix (1954) but not in the other references, although it plays an important part in the interpretation. Thus, Dainton, Fowler and Kent increase the number of Lithium nuclei from the observed value of 45 to a corrected value of 130 on the basis of an argument which involves an assumed ratio between

Lithium nuclei and particles identified as Boron nuclei in various energy intervals. In Gottstein's paper (*see* his Table IV) it is assumed in the interpretation of the data that the detection efficiency for Lithium, Beryllium and Boron is five times less than for Carbon, Nitrogen and Oxygen nuclei, if the track length is less than 500 μ, and about two times less if the track length lies between 500 μ and 3,000 μ. In both these papers, therefore, the interpretation is based on an assumed overall detection and identification efficiency which for some groups of heavy primaries lies somewhere between 20% and 50%.

Although this question of efficiency contributes to the divergence of the conclusions reached by the various authors it does not represent the main cause. In the experiments of Dainton, Fowler and Kent, of Gottstein and of Kaplon, Noon and Racette (Experiment 2) the nature and energy of the particles is determined by measurements of ionization and multiple coulomb scattering of the tracks. The discrepancy in the charge spectrum as well as the very substantial disagreement in the energy spectrum (both at low and high energy) between the results obtained in these experiments and those obtained in other experiments of different type [Kaplon, Peters, Reynolds and Ritson (1952)] can, it seems, be traced to a difficulty with the technique used in measuring multiple coulomb scattering. Since this question is of great importance also for physical problems other than those discussed here it will be treated in a separate paper to be published shortly.

REFERENCES

Bradt, H. L. and Peters, B. ..	*Phys. Rev.*, 1949, **75**, 1779; 1950 *a*, **77**, 54; 1950 *b*, **80**, 943.
Dainton, A. D., Fowler, P. H. and Kent, D. W.	*Phil. Mag.*, 1951, **42**, 317; 1952, **43**, 729.
Goldfarb, L., Bradt, H. L. and Peters, B.	*Phys. Rev.*, 1950, **77**, 751.
Gottstein, K. ..	*Naturw.*, 1953, **40**, 104; *Phil. Mag.*, 1954, **45**, 347.
Kaplon, M. F., Peters, B., Reynolds, H. L. and Ritson, D. M.	*Phys. Rev.*, 1952, **85**, 295.
——, Noon, J. H. and Racette, G. W.	*Ibid.*, 1954, **93**, 914; *ibid.* (in Press).
Stix, T. H.	*Ibid.*, 1954, **95**, 782.

SYNTHETIC EXPERIMENTS IN THE BENZOPYRONE SERIES

Part LIV. Nuclear Methylation of Simple Flavonols

By A. C. Jain and T. R. Seshadri, F.A.Sc.
(From the Department of Chemistry, University of Delhi, Delhi)

Received October 11, 1954

The nuclear methylation of quercetin has been recently reported.[1] In order to get further information that may lead to a clearer understanding of the reaction, simpler flavonols have now been investigated by the same procedure.

Attempts to effect nuclear methylation of 7-hydroxy-3-methoxy flavone have been unsuccessful. Only O-methylation took place, giving rise to 3:7-dimethoxy flavone. When galangin-3-methyl ether was methylated in this way, besides galangin di- and trimethyl ethers, one C-methylated product identical with the synthetic sample of 6-C-methyl-5-hydroxy-3:7-dimethoxy flavone (I) was obtained in about 12% yield. Using kaempferol-3:4′-dimethyl ether, three products, kaempferol-3:7:4′-trimethyl ether (m.p., 154–55°), kaempferol tetramethyl ether (m.p., 165–66°) and 6-C-methyl kaempferol-3:7:4′-trimethyl ether (II, m.p., 182–83°) have been obtained. In another experiment using excess of reagent and heating for a longer period, the trimethyl ethers were not obtained and the product consisted of a mixture of kaempferol tetramethyl ether and 6-C-methyl kaempferol tetramethyl ether (m.p., 163–64°). Methylation with methyl iodide and methanolic potash was also earlier carried out in the case of kaempferol and kaempferide by Ciamician and Silber[2] and by Waljaschko.[3] They obtained three products (m.p., 175–76°, 154–55°, 139–40°) the first two of which would appear to be identical with 6-C-methyl kaempferol-3:7:4′-trimethyl ether (II) and kaempferol-3:7:4′-trimethyl ether respectively. A fraction corresponding to the third product (139–40°) can be easily isolated even in our

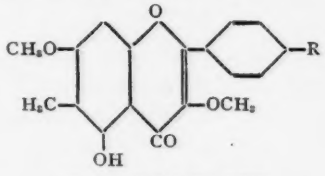

I, R = H; II, R = OCH_3

experiment. But it is found to be a mixture consisting of kaempferol tri- and tetramethyl ethers.

The preparation of reference compounds was made just as in the experiments relating to quercetin.[1] Starting with 2-hydroxy-3-methyl-ω: 4: 6-trimethoxy acetophenone (III), 8-C-methyl derivatives of galangin trimethyl ether (IV) and kaempferol tetramethyl ether (V) were obtained by two methods: (1) the Allan-Robinson condensation using the anhydride and sodium salt of benzoic or anisic acid and (2) the chalkone method using benzaldehyde or anisaldehyde and subsequent dehydrogenation. When C-methyl-ω-methoxy-phloracetophenone[1] (VI) was itself employed for the Allan-Robinson condensation, a mixture was obtained in each case, the 8-C-methyl compounds (VII) and (VIII) being the major products and the 6-C-methyl ones (IX and X) the minor. Demethylation could be conveniently effected using hydriodic acid which did not cause isomerisation under the ordinary conditions employed and the 8-C- and 6-C-methyl galangins and kaempferols obtained.

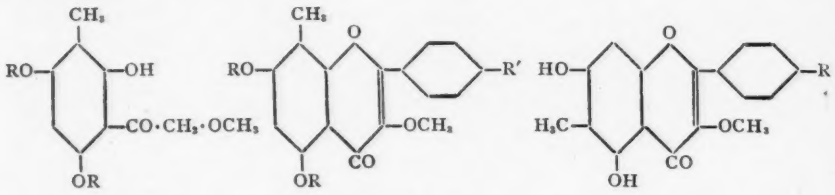

III, R=CH_3 IV, R=CH_3; R′=H V, R=CH_3; R′=OCH_3 IX, R=H

VI, R=H VII, R=R′=H VIII, R=H; R′=OCH_3 X, R=OCH_3

Recently a detailed study of the nuclear methylation of the following chromone derivatives has been made: chromones,[4,5] flavones,[5,6] flavonols,[7,1] and isoflavones.[8] In all these cases nuclear methylation has been definitely shown to take place in the 6-position. This may appear to be extraordinary because in 7-hydroxy and 5: 7-dihydroxy chromone derivatives, the 8-position is the most active in all other reactions. It is therefore obvious that the conditions of nuclear methylation are somewhat unique and are different from other reactions.

Since 3-methoxy-7-hydroxy flavone does not undergo nuclear methylation, it follows that a single hydroxyl group in the 7-position is not enough for this reaction though it is sufficient for others. The simultaneous presence of two hydroxyl groups in the 5- and 7-positions is found to be essential. This arrangement of functional groups which is the same as

present in resacetophenone seems to provide the minimum requirement of this reaction. This point has now been established by the experiments using *p*-hydroxy acetophenone and isopeonol which like peonol (*cf.*, Crabtree and Robinson[9]) do not undergo nuclear methylation. Another highly significant new observation has been made now in the case of galangin-3-methyl ether. When it is methylated with methyl iodide and methanolic sodium methoxide for a shorter period (3 hr.), 6-C-methyl galangin 3-methyl ether (IX) can be isolated as one of the products. This definitely represents the first stage of the reaction and has not so far been isolated in any other case and it supports the earlier contention of Crabtree and Robinson[9] that C-methylation should precede O-methylation of the *para*-hydroxyl group.

An earlier explanation of nuclear methylation[10] related to resorcinol derivatives and was based on analogy with the C-methylation of acetoacetic ester. The emphasis was then placed on the behaviour of the *p*-hydroxy group undergoing isomeric change to yield a ketonic form and the carbonyl group outside the nucleus was considered to exert its effect through the ring double bonds. The experiments described in this paper emphasise the need for the presence of a free *ortho*-hydroxy group also functioning by virtue of its capacity to develop ketonic properties and this is possible through the medium of hydrogen bond formation as indicated in the formulæ XI to XIV. It follows then that carbonyl compounds of resorcinol and 5:7-dihydroxy flavone derivatives function like diketones and undergo nuclear

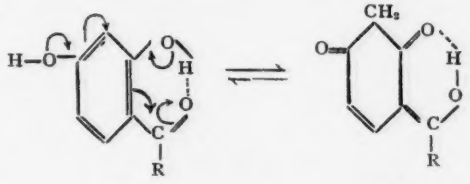

XI XII

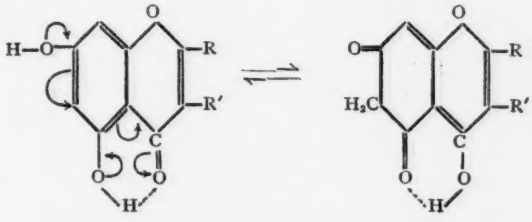

XIII XIV

methylation. The results obtained in the course of the large volume of experimental work done in the past seems to confirm the idea that the greater the capacity of the molecule to assume the ketonic form, the greater the amount of nuclear methylation. For example, phloroglucinol derivatives undergo nuclear methylation with considerable ease.

EXPERIMENTAL

8-Methyl-O-trimethyl galangin (IV)

An intimate mixture of 2-hydroxy-3-methyl-ω: 4: 6-trimethoxy acetophenone (III) (3 g.), benzoic anhydride (18 g.) and sodium benzoate (3·5 g.) was heated at 180–84° for four hours under diminished pressure, refluxed with alcoholic potash (7%, 150 c.c.) for half an hour and alcohol removed under vacuum. The remaining mixture was diluted with water and the solid product filtered and washed with water. It crystallised from dilute alcohol as colourless rectangular rods and prisms melting at 159–60° (Found: C, 69·6; H, 5·1; $C_{19}H_{18}O_5$ requires C, 69·9; H, 5·5%). A sample was also made by the chalkone method adopted by Lindstedt and Misiorny.[11] The two samples were identical and the mixed melting point was undepressed.

8-C-Methyl galangin

8-C-Methyl galangin trimethyl ether (1 g.) was refluxed with acetic anhydride (5 c.c.) and hydriodic acid (d., 1.7; 15 c.c.) for two hours and the product was poured into an ice-cold solution of sodium bisulphite and then extracted with ether. The ether solution was in turn extracted with 5% aqueous sodium carbonate and the alkaline solution neutralised. The pale yellow precipitate crystallised from methyl alcohol as yellow needles and rectangular plates melting at 262–63°. Yield, 0·5 g. (Found: C, 67·1; H, 4·1; $C_{16}H_{12}O_5$, requires C, 67·6; H, 4·2%). It yields an yellow solution with alkali and an olive brown colour turning olive green with ferric chloride. The acetate crystallised from alcohol as colourless needles melting at 183–84°.

The substance was boiled with excess of dimethyl sulphate and dry potassium carbonate in acetone medium until it gave negative ferric reaction (60 hr.). The acetone solution was filtered, concentrated and then treated with a little petroleum ether. The solid that separated crystallised from aqueous alcohol as colourless rectangular rods and prisms, melting at 159–60° alone or when mixed with an authentic sample of 8-methyl galangin trimethyl ether (IV).

Allan-Robinson Condensation of C-methyl-ω-methoxy phloracetophenone (VI) with benzoic anhydride and sodium benzoate

A well powdered mixture of the ketone (5 g.), anhydride (30 g.) and sodium salt (6 g.) was heated at 180–84° under reduced pressure and the product hydrolysed with 8% alcoholic potash, diluted with water and then saturated with carbon dioxide. The yellow solid (4·1 g.) thus obtained melted between 204–45°; it was dissolved in the minimum amount of methyl alcohol and the solution allowed to cool at room temperature. The solid that separated out was marked fraction A and that present in solution, fraction B.

Fraction A: 6-*C-Methyl*-3-*O-methyl galangin* (*IX*)

Fraction A was repeatedly crystallised from methyl alcohol; pale yellow needles and prisms, m.p. 273–74°. Yield, 1·0 g. It was acetylated by the acetic anhydride-pyridine method; the acetate crystallised from ethyl acetate-potroleum ether mixture as colourless needles melting at 167–68°. This on deacetylation with alcoholic hydrochloric acid (1 : 1) yielded pure 6-C-methyl-3-O-methyl galangin which crystallised from methyl alcohol as very pale yellow aggregates of tiny needles and prisms melting at 274·75° (Found: C, 68·1; H, 4·7; $C_{17}H_{14}O_5$ requires C, 68·5; H, 4·7%). It gives a green colour with ferric chloride and a bright yellow solution with sulphuric acid or alkali.

6-*C-Methyl galangin trimethyl ether*

The above 3-methyl ether was methylated with excess of dimethyl sulphate using potassium carbonate and acetone. The complete methyl ether crystallised from methyl alcohol as colourless rectangular needles and plates, melting at 160–61° which was depressed to 140° when mixed with the synthetic sample of 8-C-methyl galangin-trimethyl ether. (Found: C, 69·5; H, 5·9%).

6-*C-Methyl*-3 : 7-*O-dimethyl galangin* (*I*)

The 3-methoxy flavone (IX) (0·2 g.) in acetone solution was refluxed with dimethyl sulphate (0·07 c.c., 1 mole) and anhydrous potassium carbonate (0·5 g.) for 12 hours. Acetone was distilled off and water added to dissolve the potassium salts. The insoluble solid was filtered and washed with aqueous sodium carbonate and with water. It crystallised from methyl alcohol as pale yellow elongated rhombohedral prisms, melting at 165–66° (Found: C, 68·8; H, 4·8; $C_{18}H_{16}O_5$ requires C, 69·2; H, 5·1%). It is sparingly soluble in alkali and gives a green colour with alcoholic ferric

chloride. The acetate crystallised from ethyl acetate-petroleum ether mixture as colourless shining aggregates of small prisms melting at 183–84°.

6-C-Methyl galangin

The 3-methyl ether (IX) was demethylated with hydriodic acid in the usual way; the product crystallised from ethyl acetate as yellow rectangular plates melting at 228–30° (Found: C, 68·1; H, 4·1; $C_{16}H_{12}O_5$ requires C, 67·6; H, 4·2%). It dissolves in alkali or concentrated sulphuric acid to an yellow solution and yields an olive green colour with alcoholic ferric chloride. The acetate crystallised from ethyl alcohol as colourless small prisms and prismatic needles, melting at 165–66°.

Fraction B: *8-C-methyl-3-O-methyl galangin* (*VII*)

The solid (fraction B) was dissolved in the minimum amount of methyl alcohol and the solution cooled when a yellow solid (3·0 g.) (m.p., 221–26°) separated out. It was converted into its acetate which crystallised from ethyl acetate-petroleum ether mixture as colourless long prismatic needles, melting at 185–87°. The pure acetate was deacetylated by refluxing it with alcoholic hydrochloric acid (1 : 1); the product crystallised from methyl alcohol as elongated lens-shaped crystals melting at 235–37° (Found: C, 69·0; H, 4·5; $C_{17}H_{14}O_5$ requires C, 68·5; H, 4·7%). It is highly soluble in alcohol, acetone and ethyl acetate and gives a green colour with alcoholic ferric chloride. Complete demethylation with hydriodic acid and methylation in the usual way yielded 8-methyl galangin and its trimethyl ether respectively, agreeing in their behaviour with the samples prepared earlier.

8-C-Methyl-3 : 7-O-dimethyl galangin

Methylation of 8-C-methyl galangin and 8-C-methyl-3-O-methyl galangin with two moles and one mole of dimethyl sulphate respectively using dry potassium carbonate and acetone gave a solid which when crystallised twice from methyl alcohol melted at 157–58° (Found: C, 69·3; H, 5·0; $C_{18}H_{16}O_5$ requires C, 69·2; H, 5·1%). It imparts a pale green colour to alcoholic ferric chloride and is sparingly soluble in aqueous alkali. The acetate crystallised from ethyl acetate-petroleum ether mixture as colourless rectangular prisms, melting at 195–97°.

Nuclear methylation of galangin-3-methyl ether

(*a*) *Using methanolic sodium methoxide*.—To a cold solution of sodium methoxide (from 7·5 g. of sodium) in absolute methanol (200 c.c.) was added 5 : 7-dihydroxy flavonol (5 g.) and the resulting deep reddish brown

solution refluxed with methyl iodide (20 c.c.) for 3 hours. Methyl alcohol and methyl iodide were then removed under vacuum and the residue was diluted with water, acidified and extracted with ether containing a little chloroform. The extract was washed with water and evaporated to dryness. The solid left behind was extracted with 5% aqueous sodium carbonate (solid A). The sodium carbonate solution after acidification yielded a pale yellow solid (0·4 g.) which after repeated crystallisations from methyl alcohol formed pale yellow aggregates of tiny needles and melted at 273–74° alone or when mixed with an authentic sample (mentioned earlier) of 3-methoxy-5:7-dihydroxy-6-C-methyl flavone (IX); the acetates also agreed.

The solid (A) was extracted with boiling benzene to remove the completely methylated flavone and the remaining sodium salt was acidified when a pale yellow crystalline solid separated out. It was collected and crystallised from a large amount of alcohol. The first crop after further crystallisation from methanol gave a product (100 mg.) identical with 6-C-methyl-3:7-O-dimethyl galangin. The alcoholic mother liquor yielded a solid (3·5 g.) which after recrystallisation melted at 142–44° and yielded a deep brown colour with alcoholic ferric chloride. In its properties, it resembles galangin-3:7-dimethyl ether. The benzene extract yielded only galangin trimethyl ether (0·2 g.); m.p., 195–96°.

(*b*) *Using methanolic potash.*—Galangin-3-methy ether (5 g.) in methanol (75 c.c.) and methyl iodide (40 c.c.) was boiled with a solution of potassium hydroxide (8 g.) in methyl alcohol (40 c.c.), 2 c.c. added at a time during 2 days. The solvent was distilled off under reduced pressure, the residue was diluted with water and acidified. The solid that separated out was filtered, and boiled with 5% aqueous sodium carbonate (150 c.c.) for 15 minutes. The solution on acidification did not yield any crystallisable material; the undissolved solid (5·4 g.) was extracted in a soxhlet with dry benzene (Benzene solution A). The insoluble portion (1·5 g.) was boiled with dilute acid and the solid collected. Fractional crystallisation from methyl alcohol yielded two products. The sparingly soluble one (0·6 g.) was identical with 6-C-methyl-3:7-O-dimethyl galangin (I) (m.p., 165–66°; acetate, m.p. 183–84°) while the more soluble one was galangin dimethyl ether.

The benzene solution (A) was concentrated when an almost colourless solid was obtained. It crystallised from alcohol as colourless needles melting at 193–94° undepressed by an authentic sample of galangin trimethyl ether.

2-Hydroxy-3-methyl-α-:4:6:4′-tetramethyl chalkone

A mixture of 2-hydroxy-3-methyl-ω:4:6-trimethoxy acetophenone (III) (1·2 g.) and anisaldehyde (0·68 g.) was dissolved in 8% alcoholic potash

(40 c.c.) and the resulting solution was left corked at room temperature for 48 hours. It was diluted with cold water when some turbidity appeared which was removed by extraction with ether. The aqueous solution was acidified and cooled when a bright yellow product separated out. It was filtered, triturated with aqueous sodium bicrabonate and then with water. The chalkone crystallised from methyl alcohol as small yellow prisms melting at 134–35° (Found: C, 66·9; H, 5·9; $C_{20}H_{22}O_6$ requires C, 67·0; H, 6·1%). Yield, 0·8 g. It gives a reddish-brown colour with ferric chloride and an orange-red solution with concentrated sulphuric acid.

8-*C-Methyl-kaempferol tetramethyl ether* (*V*)

(i) A mixture of the above chalkone (0·5 g.) and selenium dioxide (0·5 g.) was treated with dry amyl alcohol (5 c.c.) and then refluxed at 140° for 15 hours. After cooling, it was filtered and the selenium residue on the filter paper was washed with boiling rectified spirits. Amyl alcohol was distilled off under vacuum and the last traces removed by steam distillation. The residue was washed with a little petroleum ether and then crystallised from ethyl acetate-petroleum ether mixture. 8-Methyl kaempferol tetramethyl ether separated as colourless needles, m.p. 191–92°. Yield, 0·3 g. (Found: C, 66·8; H, 5·3; $C_{20}H_{20}O_6$ requires C, 67·4; H, 5·6%).

(ii) 2-Hydroxy-3-methyl-ω: 4: 6-trimethoxy acetophenone (III) (2 g.), anisic anhydride (15 g.) and sodium anisate (2.5 g.) were condensed by the Allan-Robinson method; the product (1·5 g.) crystallised from ethyl acetate-petroleum ether mixture as colourless needles, m.p. 191–92° alone or mixed with the above sample.

8-*C-Methyl kaempferol*

The above tetramethyl ether (0·5 g.) was refluxed with hydriodic acid (d., 1·7; 8 c.c.) and acetic anhydride (5 c.c.) for 3 hours; the product crystallised from methyl alcohol as pale yellow aggregates of small needles melting at 284–86° (Found in the sample dried at 110° *in vacuo*: C, 63·9; H, 4·2; $C_{16}H_{12}O_6$ requires C, 64·0; H, 4·0%). It gives an olive brown colour with ferric chloride. The acetate crystallised from ethyl acetate-petroleum ether mixture as colourless long needles and rectangular prisms melting at 216–17°. When the tetrahydroxy flavone was re-methylated by the potassium carbonate-acetone method, the product was found to be identical with 8-C-methyl kaempferol tetramethyl ether.

Allan-Robinson Condensation of C-methyl-ω-methoxy phloracetophenone (*VI*) *with anisic anhydride and sodium anisate*

The ketone (6 g.), anhydride (36 g.) and sodium salt (6 g.) were condensed by the Allan-Robinson method and the product was fractionally crystallised

from methyl alcohol. The sparingly soluble solid melting at 268–73° was marked fraction A and the more soluble one (m.p., 208–20°) fraction B.

Fraction A: 6-*C-methyl*-3 : 4′-*O-dimethyl kaempferol* (*X*)

It was converted into its acetate which formed colourless needles and rectangular rods (m.p., 191–92°) when crystallised from ethyl acetate-petroleum ether mixutre. The acetate was hydrolysed with alcoholic hydrochloric acid (1 : 1) and the product crystallised from methyl alcohol; pale yellow needles, m.p. 276–77°. Yield, 0·85 g. (Found: C, 65·5; H, 5·1; $C_{18}H_{16}O_6$ requires C, 65·9; H, 4·9%).

6-C-Methyl-O-tetramethyl kaempferol

Compound (X) (0·1 g.) was refluxed with dimethyl sulphate (excess, 0·8 c.c.) and potassium carbonate (5 g.) until it gave negative ferric reaction (80 hours); the product crystallised from ethyl acetate-petroleum ether mixture as colourless rectangular plates melting at 163–64°. This m.p. was considerably depressed when mixed with synthetic 8-C-methyl-O-tetramethyl kaempferol (Found: C, 66·9; H, 5·4; $C_{20}H_{20}O_6$ requires C, 67·4; H, 5·6%).

6-*C-Methyl*-3 : 7 : 4′-*O-trimethyl kaempferol* (*II*)

6-C-Methyl-kaempferol dimethyl ether (X) (0·24 g.) in acetone solution (100 c.c.) was refluxed with dimethyl sulphate (0·08 c.c.) and potassium carbonate (0·5 g.) for 10 hours and the product was crystallised from ethyl acetate-petroleum ether mixture; yellow rectangular tablets melting at 182–83° (Found: C, 66·5; H, 5·0; $C_{19}H_{18}O_6$ requires C, 66·7; H, 5·3%). The acetate crystallised from alcohol as colourless rectangular rods, m.p. 199–200°.

6-C-Methyl kaempferol

The dimethyl ether (X) (0·25 g.) was refluxed with hydriodic acid (10 c.c.) and acetic anhydride (5 c.c.) for 2 hours. The 6-C-methyl kaempferol crystallised from ether-petroleum ether mixture as small yellow prisms melting at 290–91° (Found: C, 63·8; H, 4·1; $C_{16}H_{12}O_6$ requires C, 64·0; H, 4·0%). It gives a green colour with alcoholic ferric chloride and the acetate crystallised from alcohol as colourless tiny prisms, m.p. 179–80°.

Fraction B: 8-*C-methyl*-3 : 4′-*O-dimethyl kaempferol* (*VIII*)

The solid was acetylated and the product was repeatedly crystallised from alcohol when it was obtained as colourless prismatic needles and rectangular rods melting at 174–75°. It was deacetylated with alcoholic hydrochloric acid (1 : 1) and then crystallised twice from methyl alcohol;

yellow long prismatic needles, m.p. 228–29°. Yield, 2·5 g. (Found: C, 65·3; H, 4·9; $C_{18}H_{16}O_6$ requires C, 65·9; H, 4·9%). Complete demethylation and methylation in the usual way gave 8-C-methyl kaempferol and its tetramethyl ether respectively.

8-C-Methyl-O-3 : 7 : 4′-trimethyl kaempferol

The above flavone (VIII) was methylated with one mole of dimethyl sulphate as described earlier and the product was crystallised from methyl alcohol; pale yellow needles, m.p. 165–66° (Found: C, 67·0; H, 4·3). The acetate crystallised from ethyl acetate-petroleum ether mixture as colourless small prisms melting at 153–54°.

Nuclear methylation of kaempferol-3 : 4′-dimethyl ether

Methyl alcoholic solution of potassium hydroxide (18 g. in 70 c.c.) was added in lots of 2 c.c. during 12 hours to a refluxing methanolic solution of kaempferol-3 : 4′-dimethyl ether (10 g.) and methyl iodide (55 c.c.). Refluxing was continued for 12 hours more and the solvent removed under reduced pressure. The residue was treated with water and the pale yellow crystalline solid (9·2 g.) was collected. The filtrate did not yield anything on acidification. The solid was refluxed with 5% aqueous sodium carbonate (250 c.c.) for 15 minutes and the undissolved solid was filtered. The filtrate did not yield anything after acidification. The dried residue was dissolved in the minimum amount of absolute alcohol and treated with alcoholic potash (1·1 g.) when an orange potassium salt began to separate. Alcohol was removed under vacuum and the residue extracted with dry benzene (Benzene solution B). The insoluble residue (6·5 g.) was treated with hot dilute hydrochloric acid and the product was fractionally crystallised from methyl alcohol. The first crop melted at 171–76° which on twice crystallisation from ethyl acetate melted at 182–83° alone or when mixed with the synthetic sample of 6-C-methyl-3 : 7 : 4′-O-trimethyl kaempferol (II); yield 1 g. The methyl alcoholic mother liquor yielded 3 : 7 : 4′-O-trimethyl kaempferol melting at 154–55°; yield, 4·2 g.

The benzene solution (B) was concentrated and a little petroleum ether added to remove the impurities. The clear solution gave a product which melted at 162–64°. After a few crystallisations from ethyl acetate, it melted at 165–66° alone or when mixed with kaempferol tetramethyl ether; yield, 3·0 g.

Isopeonol (resacetophenone-2-methyl ether)

It was earlier obtained in a poor yield along with peonol by the Hoesch condensation of resorcinol monomethyl ether and acetonitrile[12] or by Fries migration of O-monomethyl resorcinol acetate.[13] Now it has been

prepared by partial benzoylation of the 4-hydroxy group, methylation and subsequent debenzoylation as follows: 4-O-Benzoyl resacetophenone (m.p., 107–08°) (10 g.) was refluxed in dry acetone solution with methyl iodide (30 c.c.) and anhydrous potassium carbonate (50 g.) during 30 hours on a water-bath. After removal of solvents, water was added to the residue and the resulting mixture was extracted with ether. The ether residue was kept in 8% methyl alcoholic potash (250 c.c.) at room temperature for 3 hours, refluxed for half an hour, neutralised and methyl alcohol was evaporated in vacuum. The residue was extracted with ether and the ether solution was washed with sodium bicarbonate solution and extracted with aqueous sodium hydroxide. The alkaline solution was acidified and the resulting solid crystallised from aqueous alcohol when colourless needles melting at 139–40° separated. Yield, 5·5 g. (Found: C, 64·9; H, 6·2; $C_9H_{10}O_3$ requires C, 65·1; H, 6·0%). Hoesch reported its m.p. as 137°.

Summary

3-Methoxy-7-hydroxy flavone does not undergo nuclear methylation. Nuclear methylation of (1) 3-O-methyl galangin and (2) 3:4′-O-dimethyl kaempferol has been shown to take place in the 6-position. As an intermediate in the case of (1) 3-O-methyl-6-C-methyl galangin has been isolated. The minimum structural requirements of this reaction and its mechanism are discussed.

References

1. Jain and Seshadri .. *J.S.I.R.*, 1954, **13B**, 539.
2. Ciamician and Silber .. *Ber.*, 1899, **32**, 863.
3. Waljaschko .. *Archiv. Pharm.*, 1909, **247**, 453.
4. Whalley .. *J.A.C.S.*. 1952, **74**, 5795.
5. Mukerjee and Seshadri .. *Proc. Ind. Acad. Sci.*, 1953, **38A**, 208.
6. Bannerjee and Seshadri .. *J.S.I.R.*, 1954, **13B**, 598.
7. Jain and Seshadri .. *Ibid.*, 1953, **12B**, 564.
8. Mehta, Seshadri and Varadarajan .. *Proc. Ind. Acad. Sci.*, 1953, **38A**, 381.
   Iengar, Mehta, Seshadri and Varadarajan *J.S.I.R.*, 1954, **13B**, 166.
   Mehta and Seshadri *J.C.S.*, 1954, under publication.
9. Crabtree and Robinson .. *Ibid.*, 1918, **113**, 868.
10. Seshadri and Venkateswarlu .. *Proc. Ind. Acad. Sci.*, 1941, **14A**, 297.
11. Lindstedt and Misiorny .. *Acta. Chem. Scand.*, 1951, **5**, 1213.
12. Hoesch .. *Ber.*, 1915, **48**, 1126.
13. Baker .. *J.C.S.*, 1934, 1691.

STUDIES OF GALLIC ACID COMPLEXES WITH METALS AND THEIR ANALYTICAL APPLICATIONS

Part I. Spectrophotometric Investigation

BY CH. VENKATESWARLU, M. SANKAR DAS AND V. T. ATHAVALE

(Chemistry Division, Atomic Energy Establishment, Bombay, India)

Received November 11, 1954

(Communicated by Prof. H. J. Bhabha, F.A.SC., F.R.S.)

INTRODUCTION

THERE are only a few colorimetric methods for the quantitative estimation of titanium, which are both selective and sensitive. Among the inorganic reactions,[1–4] the well-known Weller's[1] hydrogen peroxide method is widely used because of its selectivity even though it is less sensitive. The organic reagents employed successfully for the estimation are salicylic acid,[5,6] thymol,[7,8] chromotropic acid,[9–13] tiron,[14–16] disodium-1, 8 dihydroxy-3, 6 naphthalene disulfonate,[17] hydroquinone,[18] oxine,[19] ascorbic acid,[20] sulfosalicylic acid[21] and gallic acid.[22–24]

P. N. Das Gupta[22] found gallic acid to be a sensitive reagent for the detection of titanium and observed that the intensity of colour developed was proportional to the concentration of the metal. Shemyakin and collaborators[23, 24] found that this was more sensitive than the perhydrol method, but that Fe, Mo, U, W, Cr, Ce, Al, Be, Th, Zr, Mn, Zn, Ni, Co and Ca interfered in the estimation of titanium.

In the above procedures using gallic acid as a reagent, no mention was made of the effect of pH, except that the solution should be neutral. The spectrophotometric characteristics of the method have not yet been studied. Hence a systematic spectrophotometric investigation of this reaction with particular reference to the effect of pH, reagent concentration, effect of time, formula of the complex and interferences due to other metals have been undertaken and the results are presented in this paper.

REAGENTS

Gallic acid.—E. Merck, G. R. Recrystallised and dried at 120° C. Fresh solutions were prepared when required.

Titanium solution.—" Specpure " titania fused with potassium bisulphate and taken in 5% (v/v) sulphuric acid to get the required concentration of TiO_2.

Ammonium acetate.—E. Merck G. R.

Sulphuric acid.—E. Merck G. R. (sp. gr. 1·84).

Apparatus

All extinction measurements were made with Beckman DU Quartz spectrophotometer using 1 cm. quartz cells. For pH measurements, the bench type Cambridge pH meter was used.

Absorption Spectrum of Gallic Acid

Absorption spectrum of 0·001% gallic acid at different pH values between 200–320 *mμ* with hydrogen lamp was studied and the results are recorded in Table I.

Table I

Absorption data of gallic acid between 200–320 *mμ with hydrogen lamp*

pH	$\lambda_{max.}$ *mμ*	Molecular extinction coefficient $E_{max.}$	$\lambda_{max.}$ *mμ*	Molecular extinction coefficient $E_{max.}$
1·2	216	27049	271	9696
1·8	215	27203	271	9696
4·4	213	28053	263	8234
5·2	..	..	260	7809
6·5	212	25416	259	8234

This shows an absorption peak at 271 *mμ* with a molecular extinction coefficient 9696 which remains constant at pH 2·0 and below. With increase of pH, the peak shifts towards lower wave-length, which is in good agreement with the general observations of Mattil and Filer.[25] In addition, another peak is found at 216 *mμ*.

The absorption spectrum of gallic acid with different concentration was also investigated between 300 and 500 *mμ* (Fig. 1) with a tungsten lamp and the results are recorded in Table II.

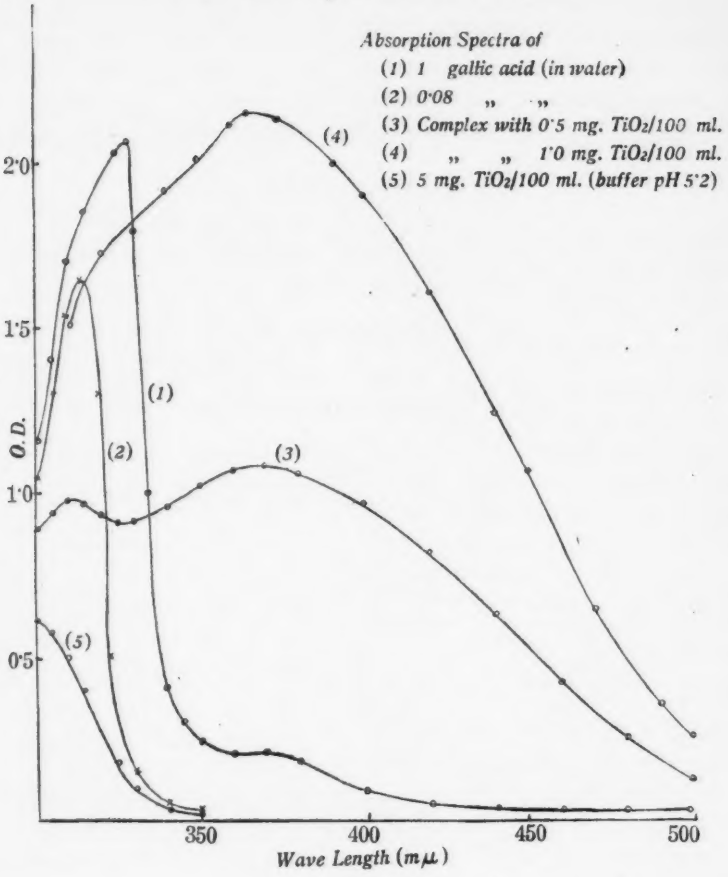

FIG. 1

TABLE II

Absorption data of gallic acid between 300 and 500 mμ with tungsten lamp

Concentration of gallic acid	pH	$\lambda_{max.}$ mμ	Molecular extinction coefficient $E_{max.}$
1·0%	2·8	327	35·4
0·08%	3·4	314	344·2
0·08%	5·2	307	265·6

It is evident from Table II that the absorption peak in this region shifts towards higher wave-length with increase of concentration. When the same concentration was used, increase of pH shifts the peak towards lower wave-length. This might be due to difference of ionization of gallic acid under different conditions.

Absorption Spectrum of the Ti-Gallic Acid Complex

For the preparation of the complex, 0·5 and 1·0 mg. of TiO_2 were taken in two different 100 ml. flasks, 20 and 40 mg. of gallic acid respectively were added, and then the necessary amount of ammonium acetate to give a pH of 5·2 when the solution was made upto 100 ml. The spectra of these solutions studied between 300 and 600 *mμ* with tungsten lamp, are shown in Fig. 1. With the complex containing 0·5 mg. TiO_2, two absorption peaks were observed at 311 and 370 *mμ*. With that of 1·0 mg. TiO_2 the nature of spectrum was the same except that below 340 *mμ* instead of an absorption peak at 311 *mμ*, there is an abrupt change in the slope at 315 *mμ*. It was shown above that the absorption peak of gallic acid in the region 300–330 *mμ* exhibits a shift towards higher wave-length with increase of concentration. When more gallic acid was used for the corresponding increase of TiO_2, the high extinction of the corresponding blank might be compensating the comparatively small increase in extinction of the complex in this region. The complex was prepared with 0·05 mg. TiO_2 and 2·5 mg. gallic acid in 100 ml. and its spectrum between 200–320 *mμ* (Fig. 2) was studied with hydrogen lamp. The absorption peaks of gallic acid, *viz.*, 213 and 260 *mμ*, were shifted to 231 and 293 *mμ* respectively showing the formation of a true complex between Ti (IV) and gallic acid under these experimental conditions. The absorption spectra of titanium solutions under these experimental conditions are shown in Figs. 1 and 2. These spectra were studied immediately after preparation of the solutions to avoid hydrolysis.

Effect of pH

Since gallic acid deteriorates readily in alkaline solutions due to absorption of oxygen from atmosphere, the study of the effect of pH on this complex had to be restricted below pH 7·0. 1 ml. of titanium solution (0·25 mg. TiO_2) and 15 mg. gallic acid were taken in a number of 100 ml. flasks and varying amounts of ammonium acetate solution were added. The solutions were made up to 100 ml., pH measured, and the extinction at 370 *mμ* taken. A plot of the optical density against pH (Fig. 3) showled that colour development reached a maximum at pH 4·2 and remained constant at higher pH. A convenient pH of $5{\cdot}2 \pm 0{\cdot}05$ could be had by keeping the ratio of

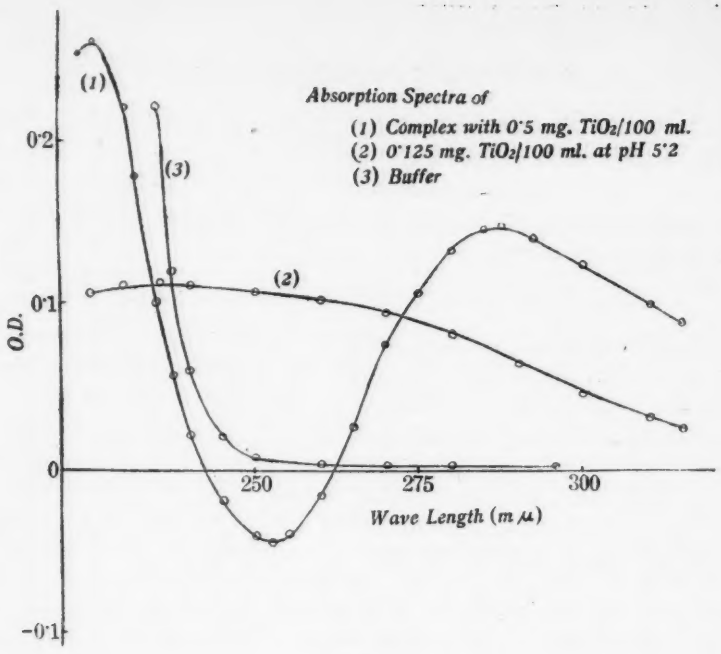
Absorption Spectra of
(1) Complex with 0·5 mg. TiO2/100 ml.
(2) 0·125 mg. TiO2/100 ml. at pH 5·2
(3) Buffer
(1)
(2)
(3)
0·2
0·1
0
-0·1
O.D.
250
275
300
Wave Length (mμ)

FIG. 2

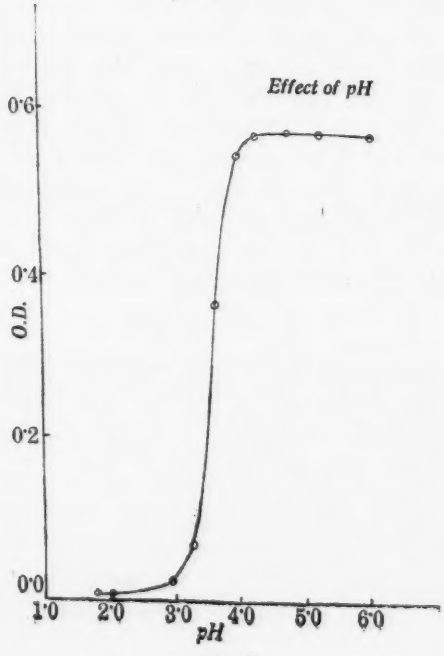
Effect of pH
0·6
0·4
0·2
0·0
O.D.
1·0
2·0
3·0
4·0
5·0
6·0
pH

FIG. 3

5% (v/v) sulphuric acid to 2 N ammonium acetate solution at 1 : 5. Ammonium acetate had practically no absorption at this wave-length.

Effect of Gallic Acid Concentration

The effect of gallic acid concentration was studied with 0·5, 0·25 and 0·05 mg. TiO_2 per 100 ml. The results are shown in Fig. 4 *a, b, c*. The optical densities were measured again after 24 hours. The curves show that:

(1) A complex is formed, which slowly transformed into another when more gallic acid was available. Further increase showed no other complex formation, slight slope of the curve after colour saturation being due to excess gallic acid.

(2) Higher gallic acid ratio was required for colour saturation with lower TiO_2 concentration, showing that the complex formation is perhaps a reversible reaction.

From solutions with 0·5 mg. TiO_2 and less than 0·5 mg. gallic acid, a precipitate was obtained on keeping.

Empirical Formula of the Complex

Job's method of continuous variation[26] was applied for the determination of the empirical formula of the complex using $1{\cdot}8\times10^{-3}$ molar solutions of gallic acid and titanium. The ionic strength of the solutions was

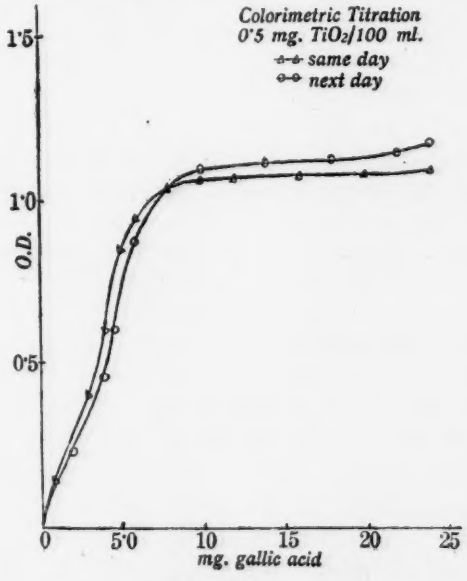

Fig. 4 (*a*)

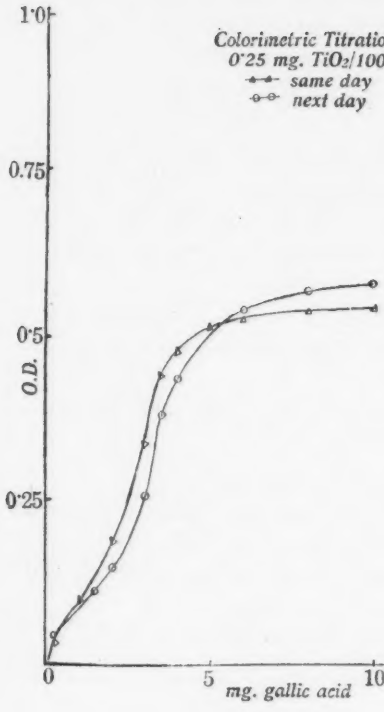

FIG 4 (*b*)

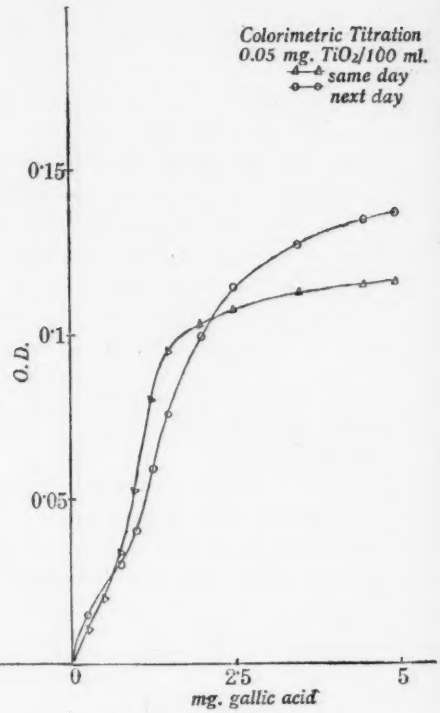

FIG. 4 (*c*)

maintained by keeping sulphuric acid and ammonium acetate concentrations constant. The plot of the difference between the observed extinction values and the expected ones if there were no reaction, against the composition at 295 and 370 $m\mu$ showed the complex to correspond to TiR_6 which was further confirmed with $2{\cdot}5\times10^{-3}$ molar solutions (Fig. 5). To determine the composition of the other complex, indicated in colorimetric titrations, the extinction values were measured at 237, 260, 285 and 335 $m\mu$, but the same complex, *viz.*, TiR_6, was found showing that it was obviously stabler than the other ones[27]. At 260 $m\mu$, the corrected extinction values were negative because the extinction of the reagent was more than that of the complex.

Further work is under progress to establish the composition of the less stable complex.

ESTIMATION OF TITANIUM

The amount of reagent and the wave-length to be employed for different concentrations of titanium are given in Table III. In all cases the pH was

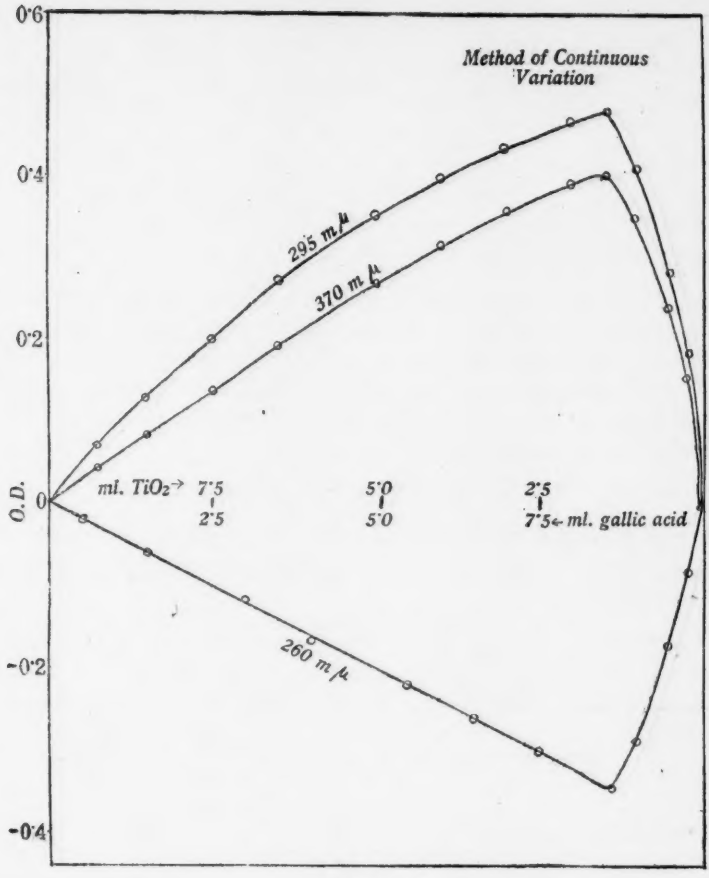

FIG. 5.

adjusted to 5·2. It was found that Beer's law was obeyed at all wave-lengths investigated. Even after keeping the solutions for a day, there was no appreciable difference in the extinction values. More than 10 mg. TiO_2/100 ml. was not tried as it can be easily estimated gravimetrically with tannin.

INTERFERENCE

Interference due to most of the metals reported earlier[24] was eliminated readily by the addition of ammonium tartrate and then adjusting pH to 5·2 in the above procedure. Tartrate, itself, does not interfere in the estimation. Phosphate interfered by giving a precipitate. Oxalate and citrate reduced

TABLE III

Concentration of titanium mg. TiO_2/100 ml.	Quantity of gallic acid mg.	Wave-length $m\mu$
0·01 to 0·1	10–15	295 or 370
0·1 to 1·0	50–100	370 to 450
1·0 to 10·0	400–500	500 to 550

the intensity of the colour, which might be due to the higher stability of their complexes (colourless) than the gallic acid complex. Iron, Vanadium and Molybdenum developed dark colours both in the presence and absence of tartrate. Tungsten gave higher values at 370 $m\mu$ but at 450 $m\mu$ there was no interference at all. Other methods of eliminating the interference of Fe, Mo and V are under further investigation.

SENSITIVITY OF THE METHOD

A comparison of the sensitivities[12] of the important methods with the present one given in Table IV, shows that the method described here is more sensitive than the others.

TABLE IV

Comparison of sensitivity of the method

Reagent	Wave-length $m\mu$	Extinction for 1 μg. Ti/ml. for an optical depth of 1 cm.
Hydrogen peroxide ..	410	0·0155
Thymol	425	0·11
Tiron	410	0·28
Chromotropic acid ..	420	0·38
Gallic acid	370	0·35
Gallic acid ..	295	0·48

SUMMARY

The reaction between Ti (IV) and gallic acid was spectrophotometrically investigated, with particular reference to the effect of pH, effect of reagent concentration and interferences. An orange coloured complex, formed between pH 4·2 and 6·0, was employed for estimation of titania varying

from 0·01 mg. to 10·0 mg. per 100 ml. The formula of the complex was found to be TiR_6. The chief advantages of the procedure are that Beer's law is obeyed at all wavelengths investigated, and that it is rapid and highly sensitive, the colour being stable for 24 hours.

ACKNOWLEDGEMENT

The authors consider it their pleasant duty to thank Mr. M. Sundaresan for his constructive criticism and Dr. J. Shankar for his keen interest during the progress of this work.

REFERENCES

1. Weller .. *Ber.*, 1882, **15**, 2593.
2. Denise Delabosse .. *Compt. rend.*, 1953, **236**, 2313.
3. Kokorin, A. I. .. *Zevodskaya Lab.*, 1950, **16**, 777.
4. Susumu Suzuki .. "Ichiro Okawa and Sei Uemura," *J. Chem. Soc. Japan, Pure Chem. Sect.*, 1951, **72**, 49.
5. Muller .. *J. Am. Chem. Soc.*, 1911, **33**, 1506.
6. Max Schenk .. *Helv. Chim. Acta*, 1936, **19**, 1127.
7. Victor Lenher and Crawford, W. G. *J. Am. Chem. Soc.*, 1913, **35**, 138.
8. John, V. G. and Robinson, R. J. *Anal. Chem.*, 1951, **23**, 1871.
9. Geissow .. *Munich Dissertation*, 1902.
10. Endredy, A. V. and Fr. Brugger *Z. anorg. allgem. Chem.*, 1942, **249**, 263.
11. Rosotte, R. and Jaudon, E. .. *Anal. Chim. Acta*, 1952, **6**, 149.
12. Ovenston, T. C. J., Parker, C. A. and Hatchard, C. G. *Ibid.*, 1952, **6**, 7.
13. Sinyakova, S. I. and Ivanov, N. P. *Zhur. Anal. Khim.*, 1952, **7**, 349.
14. Yoe, J. H. and Armstrong, A. R. *Science*, 1945, **102**, 207.
15. ——— .. *Anal. Chem.*, 1947, **19**, 100.
16. Harvey, A. E., Jr. and Manning, D. L. *J. Am. Chem. Soc.*, 1952, **74**, 4744.
17. Max Zimmerman .. *Z. Erzbergbau u. Metallhuttenw.*, 1952, **5**, 148.
18. Johnson, C. M. .. *Iron Age.*, 1946, **157**, No. 14, 66.
19. Gardner, K. .. *Analyst*, 1951, **76**, 485.
20. Edward Hines and Boltz, D.F. *Anal. Chem.*, 1952, **24**, 947.
21. Max Zeigler and Oskar Glemser *Z. anal. chem.*, 1953, **139**, 92.
22. Das Gupta, P. N. .. *J. Ind. Chem. Soc.*, 1929, **6**, 855.
23. Shemyakin, F. M. .. *Zavodskya Lab.*, 1934, **3**, 1090.
24. —— and Neumolotova, A. *J. Gen. Chem.* (*U.S.S.R.*), 1935, **5**, 491.
25. Mattil, K. F. and Filer, L. J. Jr. *J. Ind. and Eng. Chem., Anal. Edn.*, 1944, **16**, 427.
26. Job .. *Ann. Chim.*, 1928, **9** (10), 113.
27. Vosburgh, W. C. and Cooper, G. R. *J. Am. Chem. Soc.*, 1941, **63**, 437.

1609-54 Printed at The Bangalore Press, Bangalore City, by C. Vasudeva Rao, Superintendent, and Published by The Indian Academy of Sciences, Bangalore.

INDEX TO VOL. XL (A)

AUTHOR INDEX

Anantakrishnan, S. V. .. *See* Mathai and Anantakrishnan.
See Padmanabhan and Anantakrishnan.

Ananthakrishnan, R. .. Prominence activity (1905–1952), 72.

Athavale, V. T. .. *See* Venkateswarlu and others.

Balakrishna, S. .. Effect of temperature on ultrasonic velocities in some Indian rocks, 125.

Daniel, R. R. and Pal, Yash — An abnormal τ-meson decay, 114.

Daniel, R. R., Friedmann, G., Lal, D., Pal, Yash and Peters, B. — On the construction of large nuclear emulsion block detectors, 151.

Das, M. Sankar .. *See* Venkateswarlu and others.

Dube, G. P. and Singh, Lal Saheb — On the semi-empirical mass formula and alpha disintegration energy in the region of heavy and medium heavy nuclides, 37.

Friedmann, G. .. *See* Daniel and others.

Iyengar, S. B. D. .. *See* Ramanna and Iyengar.

Jain, A. C. and Seshadri, T. R. — Synthetic experiments in the benzopyrone series, LIV, 249.

Jayaraman, A. .. *See* Raman and Jayaraman.

Karkhanavala, M. D. and Shankar, J. — An X-ray study of natural monazite, I, 67.

Krishnamurti, D. .. The Raman spectrum of diamond, 211.

Krishnan, R. S., Narayanan, P. S. and Sivarajan, S. R. — Elliptic polarisation of light scattered by colloidal solutions, 140.

Lal, D. .. *See* Daniel and others.

Mani, G. S. and Pandhi, R. — Angular distribution of protons emitted in the reaction $_7N^{14}(\alpha, p)_8O^{17}$, 61

Mathai, I. M. and Anantakrishnan, S. V. — Kinetics of the olefine-bromine reaction, VII, 47.

Kinetics of the olefine-bromine reaction, VIII, 91.

Murty, D. S. R. .. North-south asymmetry of cosmic rays, 96.

Narasimhamurty, T. S. .. Photoelastic studies of optically active crystals. $NaClO_3$ and $NaBrO_3$, 167.

Narayanan, P. S. .. *See* Krishnan and others.

Padmanabhan, V. S. and Anantakrishnan, S. V. — The role of solvent in chemical reactions, I, 132.

Pal, Yash .. *See* Daniel and Pal.
See Daniel and others.

Pancharatnam, S. .. On the pleochroism of amethyst quartz and its absorption spectra, 196.

Pandhi, R. .. *See* Mani and Pandhi.

Patani, M. J. .. *See* Trivedi and Patani.

Peters, B. .. *See* Daniel and others.
The flux of primary cosmic ray nuclei of atomic number $Z \geqslant 2$ at geomagnetic latitude 30°, 230.

Raman, C. V. and Jayaraman, A. .. X-ray studies on polycrystalline gypsum, 57.
X-ray study of fibrous quartz, 107.
The structure of amethyst quartz and the origin of its pleochroism, 189.
On the structure of amethyst and its genesis in nature, 221.

Raman, C. V. and Ramdas, A. K. — The structure and optical behaviour of iridescent calcite, 1.

Ramanna, R. and Iyengar, S. B. D. — On the distribution of thermal neutrons from a fast neutron source placed at the interface of two media, 8.

Ramaseshan, S. .. A magneto-optic method for the determination of piezo-optic coefficients, 184.

Ramdas, A. K. .. *See* Raman and Ramdas.
Some illustrations of the optical behaviour of iridescent calcite, 217.

Rao, C. Lakshman, Sharma, Hari D. and Shankar, Jagdish — Different oxidation states of manganese produced by the Fe (n, p) Mn reaction, 102.

Rastogi, R. G. .. Intermediate layers of ionisation between the E and F_1 layers of the ionosphere over Ahmedabad (23° N., 72°·6 E.), 158.

Seshadri, T. R. .. *See* Jain and Seshadri.

Seth, B. R. .. Generalized singular points with applications to flow problems, 25.

Shankar, J.	..	*See* Karkhanavala and Shankar. *See* Rao and others.
Sharma, H. D.	..	*See* Rao and others. *See* Krishnan and others.
Singh, Lal Saheb	..	*See* Dube and Singh.
Sivarajan, S. R.	..	*See* Krishnan and others.
Subbaram, M. R.	..	Heterocyclic compounds, II, 22.
Sundaram, V.	..	Light scattering in soap-solvent systems—depolarisation factors of transversely scattered light in sodium oleate-xylene systems during and after gel-formation, 176.
Tillu, Mahadeo M.	..	Rapid determination of uranium in complex minerals like samarskite, columbite-tantalite and titaniobates,I, 110.
Trivedi, A. K. M. and Patani, M. J.		Distribution of electrolytes across a semi-permeable membrane in the presence of arsenic trisulphide sol, 119.
Venkateswarlu, Ch., Das, M. Sankar and Athavale, V. T.		Studies of gallic acid complexes with metals and their analytical applications, I, 260.

TITLE INDEX

Amethyst, on the structure, and its genesis in nature (Raman and Jayaraman), 221.

Amethyst quartz, on the pleochroism, and its absorption spectra (Pancharatnam), 196.

Amethyst quartz, the structure, and the origin of its pleochroism (Raman and Jayaraman), 189.

Benzopyrone series, synthetic experiments, LIV (Jain and Seshadri), 249.

Calcite, iridescent, optical behaviour, some illustrations (Ramdas), 217.

Calcite, iridescent, the structure and optical behaviour (Raman and Ramdas), 1.

Cosmic ray nuclei of atomic number $Z \geqslant 2$ at geomagnetic latitude 30°, primary, flux (Peters), 230.

Cosmic rays, North-South asymmetry (Murty), 96.

Electrolytes, distribution, across a semi-permeable membrane in the presence of arsenic trisulphide sol (Trivedi and Patani), 119.

Gallic acid complexes, studies, with metals and their analytical applications, I (Venkateswarlu and others), 260.

Gypsum, polycrystalline, X-ray studies (Raman and Jayaraman), 57.

Heterocyclic compounds, II (Subbaram), 22.

Ionosphere over Ahmedabad (23° N., 72°·6 E.), E and F_1 layers, intermediate layers of ionisation between (Rastogi), 158.

Light scattering in soap-solvent systems—depolarisation factors of transversely scattered light in sodium oleate-xylene systems during and after gel-formation (Sundaram), 176.

Manganese produced by the Fe (n, p) Mn reaction, different oxidation states (Rao and others), 102.

Mass-formula, semi-empirical, and alpha-disintegration energy in the region of heavy and medium heavy nuclides (Dube and Singh), 37.

τ-meson decay, abnormal (Daniel and Pal), 114.

Monazite, natural, an X-ray study, I (Karkhanavala and Shankar), 67.

Nuclear emulsion block detectors, large, on the construction (Daniel and others), 151.

Olefine-bromine reaction, kinetics, VII, VIII (Mathai and Anantakrishnan), 47, 91.

Photoelastic studies of optically active crystals. $NaClO_3$ and $NaBrO_3$ (Narasimhamurty), 167.

coefficients, determination, a magneto-optic method (Ramaseshan), 184.

Polarisation, elliptic, of light scattered by colloidal solutions (Krishnan and others), 140.

Prominence activity (1905–1952) (Ananthakrishnan), 72.

Protons emitted in the reaction $_7N^{14}$ $(\alpha, p)_8$ O^{17}, angular distribution (Mani and Pandhi), 61.

Quartz, fibrous, X-ray study (Raman and Jayaraman), 107.

Raman spectrum of diamond (Krishnamurti), 211.

Singular points, generalized, with applications to flow problems (Seth), 25.

Solvent, the role, in chemical reactions, I (Padmanabhan and Anantakrishnan, 132.

Thermal neutrons, on the distribution, from a fast neutron source placed at the interface of two media (Ramanna and Iyengar), 8.

Ultrasonic velocities in some Indian rocks, effect of temperature (Balakrishna), 125.

Uranium in complex minerals like Samarskite, columbite-tantalite and titaniobates, rapid determination I, (Tillu), 110.

NOTICE TO AUTHORS

Scientific papers intended for publication in the *Proceedings of the Indian Academy of Sciences* can be accepted only when they are communicated by a Fellow of the Academy whose duty shall be to satisfy himself that such communications are fit to be read at the Meeting of the Academy and published in its *Proceedings*.

Papers should not ordinarily exceed fifty pages of foolscap. MSS. should be either typewritten or written in legible hand on one side of the paper. All papers should be carefully revised by the authors and should be absolutely in final form for printing. Position for text-figures should be indicated. Each paper shall conclude with a critical summary not exceeding 350 words.

Drawings, diagrams or other illustrations should be made on larger scale (preferably) twice the size than the ones in which they are intended to appear. They should be done in Indian ink on bristol board with lettering in pencil. Scale of magnification of camera lucida tracings should be indicated by the side of drawings. In certain special cases arrangements will also be made for monochrome lithographic and other colour plates. Reduction of illustrations desired should be indicated in pencil. Appropriate legends should accompany all drawings. Names of authors are to be marked in pencil on the left-hand corner of drawing sheets. Photomicrographs should be securely mounted with colourless paste.

All tables, quotations and footnotes which will be set hereafter (beginning from Vol. I, No. 2) in types smaller than the text, should be typewritten on separate sheets and placed with the text in proper sequence. Footnotes should be numbered in Arabic numerals.

References to literature in the text should be given, whenever possible, in chronological order, only the names of authors and years of publication, in brackets, being given. They should be cited in full after the summary, the authors' names following in alphabetical order. Thus,

Name or Names of author; Name of Journal (abbreviation) with a single underline; Year of publication; Number of Volume with a double underline, and lastly page. The following would be a useful illustration:—

Bergmann and Stather . . . . . Z. Physiol. Chem., 1926, 152, 189.

Two copies of slip-proof and wherever possible, a page proof for final revision will be sent to authors. All corrections are best made on the slip-proof which should be transmitted to the Office of the Academy. All proof corrections involve heavy expenses which would be negligible if the papers are carefully revised by the authors before submission.

Authors will be supplied with reprints of their papers at cost price, if intimation is given at the time of returning the slip-proof.

Blocks appearing in the *Proceedings* will be available for purchase by their respective authors. Orders for the same should be sent along with the corrected proofs and in any case not later than one month after the date of publication of the paper. The price charged would be 25% of the actual cost of the blocks *plus* freight and despatching charges. If the blocks are reproduced in other journals or publications, due acknowledgment should be made in them to the *Proceedings*.

The original drawings and plates of blocks appearing in the *Proceedings* will be returned to such of the authors as may require them provided the cost of despatching such originals is borne by them.

CONTENTS

PAGE

On the Structure of Amethyst and its Genesis in Nature . . . . . Sir C. V. Raman and A. Jayaraman 221

The Flux of Primary Cosmic Ray Nuclei of Atomic Number $Z \geqslant 2$ at Geomagnetic Latitude 30° . . . . . B. Peters 230

Synthetic Experiments in the Benzopyrone Series. Part LIV. Nuclear Methylation of Simple Flavonols . . . A. C. Jain and T. R. Seshadri 249

Studies of Gallic Acid Complexes with Metals and their Analytical Applications. Part I. Spectrophotometric Investigation . . . . . Ch. Venkateswarlu, M. Sankar Das and V. T. Athavale 260